



This is a post-peer-review, pre-copyedit version of an article published in *Plant Journal*. The final authenticated version is available online at: <https://doi.org/10.1111/tpj.14347>

The MYB transcription factor EMA1 stimulates emission of methyl anthranilate from *Medicago truncatula* hairy roots

Jacob Pollier^{1,2}, Nathan De Geyter^{1,2}, Tessa Moses^{1,2,†}, Benoît Boachon³, José Manuel Franco Zorrilla⁴, Yuechen Bai^{1,2}, Elia Lacchini^{1,2}, Azra Gholami^{1,2}, Robin Vanden Bossche^{1,2}, Danièle Werck-Reichhart³, Sofie Goormachtig^{1,2} and Alain Goossens^{1,2,*}

¹Ghent University, Department of Plant Biotechnology and Bioinformatics, Technologiepark 71, B-9052 Ghent, Belgium

²VIB Center for Plant Systems Biology, Technologiepark 71, B-9052 Ghent, Belgium

³Institut de Biologie Moléculaire des Plantes, Unité Propre de Recherche 2357 du Centre National de la Recherche Scientifique, Université de Strasbourg, 67000 Strasbourg, France.

⁴Genomics Unit, Centro Nacional de Biotecnología-CSIC, 28049 Madrid, Spain

*For correspondence (Tel. +32 9 331 38 51; fax +32 9 331 38 09; e-mail alain.goossens@psb.vib-ugent.be).

†Present address: TM, School of Biological Sciences, University of Edinburgh, Roger Land Building, Alexander Crum Brown Road, Edinburgh EH9 3FF, UK

Corresponding author:

Alain Goossens

VIB Center for Plant Systems Biology

Ghent University, Department of Plant Biotechnology

Technologiepark 927

B-9052 Ghent (Belgium)

Tel.: +32 9 3313851; Fax: +32 9 3313809; E-mail: alain.goossens@psb.vib-ugent.be

Running title: Emission of methyl anthranilate by *Medicago*

Keywords: Volatile organic compounds, MYB transcription factor, PLATZ transcription factor, methyl anthranilate, methyl transferase, *Medicago truncatula*, jasmonate signaling

SIGNIFICANCE STATEMENT

Volatiles play an important role in the interaction of a plant with its environment. Here, we have identified a MYB transcription factor that is involved in the emission of the volatile compound methyl anthranilate in the model legume *Medicago truncatula*.

SUMMARY

Plants respond to herbivore or pathogen attacks by activating specific defense programs that include the production of bioactive specialized metabolites to eliminate or deter the attackers. Volatiles play an important role in the interaction of a plant with its environment. Through transcript profiling of jasmonate-elicited *Medicago truncatula* cells we identified Emission of Methyl Anthranilate (EMA) 1, a MYB transcription factor that is involved in the emission of the volatile compound methyl anthranilate when expressed in *M. truncatula* hairy roots, giving them a fruity scent. RNA-Seq analysis of the fragrant roots revealed the upregulation of a methyltransferase that was subsequently characterized to catalyze the *O*-methylation of anthranilic acid and was hence named *M. truncatula* Anthranilic Acid Methyl Transferase (MtAAMT) 1. Given that direct activation of the *MtAAMT1* promoter by EMA1 could not be unambiguously demonstrated, we further probed the RNA-Seq data and identified the repressor protein *M. truncatula* Plant AT-rich sequence and Zinc-binding (MtPLATZ) 1. EMA1 binds a tandem repeat of the ACCTAAC motif in the MtPLATZ1 promoter to transactivate gene expression. Overexpression of *MtPLATZ1* in transgenic *M. truncatula* hairy roots led to transcriptional silencing of *EMA1*, indicating that MtPLATZ1 may be part of a negative feedback loop to control the expression of *EMA1*. Finally, exogenous methyl anthranilate application boosted *EMA1* and *MtAAMT1* expression dramatically, thus also revealing a positive amplification loop. Such positive and negative feedback loops seem to be a norm rather than an exception in the regulation of plant specialized metabolism.

INTRODUCTION

Because of their sessile nature, plants are often confronted with various biotic and abiotic stress situations. To respond to these stresses, plants activate specific defense programs that include the production of specialized metabolites to eliminate or deter attackers. Often, these compounds are also toxic to the plants themselves or impose a metabolic cost for their production, hence their biosynthesis is strictly regulated, both spatially and temporally, to optimize plant survival under normal or stress conditions. A fundamental role in the signaling cascade that regulates plant specialized metabolism is performed by the jasmonates (JAs), ubiquitous oxylipin-derived phytohormones that also play essential roles in the regulation of many developmental and growth processes (De Geyter *et al.*, 2012; Wasternack and Strnad, 2018). The mechanisms of JA perception and primary signal transduction are generally well understood (Wasternack and Hause, 2013; Chini *et al.*, 2016; Goossens *et al.*, 2016; Wasternack and Song, 2017), however, knowledge on the connection between the primary signal transduction machinery and the onset of the specialized metabolism remains fragmented. Basic helix-loop-helix (bHLH) transcription factors, such as MYC2, are considered key in the primary JA signaling cascade, and have been shown to play a direct role in the regulation of the biosynthesis of a variety of specialized metabolites. Nonetheless, it has also become clear that regulation of specialized metabolism is subject to complex combinatorial transcriptional control by transcription factors from diverse families (De Geyter *et al.*, 2012; Chezem and Clay, 2016; Zhou and Memelink, 2016; Goossens *et al.*, 2017; Colinas and Goossens, 2018).

A specific class of plant specialized metabolites that may serve both as direct and indirect defense compounds are the volatile organic compounds (VOCs), which are lipophilic liquids with a low molecular weight and a high vapor pressure at ambient temperatures (Huang *et al.*, 2012; Mithöfer and Boland, 2012; Dudareva *et al.*, 2013; Boachon *et al.*, 2015). As direct defense compounds, VOCs may act as repellents or toxic agents against herbivores or may inhibit the growth of pathogens (Mithöfer and Boland, 2012; Dudareva *et al.*, 2013). As indirect defense compounds, plants may produce VOCs to attract carnivorous enemies of the herbivores attacking the plants or to induce anti-herbivore responses in neighboring plants (Gols, 2014;

Pierik *et al.*, 2014; Ponzio *et al.*, 2014). The release of VOCs from plants is tightly regulated, mainly at the transcriptional level, where orchestrated regulation of gene expression leads to emission of herbivore-induced volatiles (Kant *et al.*, 2004; Dudareva *et al.*, 2013; Muhlemann *et al.*, 2014). The concerted regulation of entire biosynthetic pathways implies that transcription factors contribute to the regulation of the expression of genes encoding the VOCs' biosynthetic enzymes. To date, several transcription factors involved in the regulation of the biosynthesis of VOCs have been identified. In petunia, the ODORANT1 (ODO1) R2R3-MYB transcription factor was identified as a key regulator of floral scent biosynthesis and shown to control the floral shikimate pathway towards volatile benzenoids and phenylpropanoids (Verdonk *et al.*, 2005). The ODO1 transcription factor is regulated by another R2R3-MYB transcription factor, EMISSION OF BENZENOID II (EOBII), which in addition to ODO1 and its downstream targets also regulates the VOC biosynthetic gene *isoeugenol synthase* (Spitzer-Rimon *et al.*, 2010; Van Moerkercke *et al.*, 2011). Another R2R3-MYB transcription factor, EOBI, which is also directly activated by EOBII, controls the expression of benzenoid biosynthesis genes and can activate the expression of *ODO1*. Furthermore, *EOBI* expression is negatively affected by ODO1, suggesting the existence of a negative feedback loop in the regulation of VOC emission from petunia (Spitzer-Rimon *et al.*, 2012). In contrast to ODO1, EOBI and EOBII that act as transcriptional activators, the *Petunia × hybrida* R2R3-MYB4 (PhMYB4) transcription factor represses the expression of the phenylpropanoid gene *cinnamate-4-hydroxylase*, thereby controlling metabolite flux towards the *p*-coumaric acid-derived VOCs eugenol and isoeugenol in petunia flowers (Colquhoun *et al.*, 2011). Together, these transcription factors constitute a complex transcriptional regulatory network that controls the emission of VOCs from petunia flowers. Such complex transcriptional networks are likely conserved across the plant kingdom to regulate various branches of the phenylpropanoid pathway. For instance, FaEOBII, the strawberry (*Fragaria × ananassa*) ortholog of the petunia EOBII, regulates the production of eugenol in ripe strawberry fruit receptacles (Medina-Puche *et al.*, 2015). In addition, the Arabidopsis ODO1 orthologue MYB99 was shown to act with the Arabidopsis EOBI and EOBII orthologues MYB21 and MYB24 in a regulatory triad that controls anther phenylpropanoid production in Arabidopsis (*Arabidopsis thaliana*) (Battat *et al.*, 2019).

Knowledge on regulatory networks for other classes of VOCs, such as terpenes, remains limited but individual transcription factors regulating expression of genes encoding enzymes involved in volatile terpene biosynthesis have been reported. In Arabidopsis, the AUXIN RESPONSE FACTOR 6 (ARF6) and ARF8 induce JA production, thereby triggering *MYB21* and *MYB24* expression. Together, the latter transcription factors promote nectary development and the resulting production of volatile sesquiterpenes (Reeves *et al.*, 2012). Also Arabidopsis MYC2 directly binds and activates the promoters of two sesquiterpene synthase genes, thereby promoting emission of volatile sesquiterpenes (Hong *et al.*, 2012). In addition, transcription factors regulating volatile terpene biosynthesis have been reported in orange fruit and spearmint (Li *et al.*, 2017b; Reddy *et al.*, 2017).

The legume *Medicago truncatula* serves as a model plant species for the study of two types of plant specialized metabolites, the triterpene saponins and the (iso)flavonoids (Gholami *et al.*, 2014). Also in *M. truncatula* JAs play an essential role in the regulation of specialized metabolism. This is evidenced by the increased accumulation of triterpene saponins and specific isoflavonoids in *M. truncatula* cell cultures triggered with methyl JA (Suzuki *et al.*, 2002; Broeckling *et al.*, 2005; Suzuki *et al.*, 2005; Naoumkina *et al.*, 2007). To date, only little is known about the regulators involved in JA-mediated regulation of specialized metabolism in *M. truncatula*. The RING membrane-anchor (RMA)-like E3 ubiquitin ligase Makibishi1 (MKB1) was shown to recruit the ER-associated protein degradation (ERAD) system to degrade 3-hydroxy-3-methylglutaryl-CoA reductase (HMGR), a key rate-limiting enzyme in the triterpene saponin biosynthetic pathway (Pollier *et al.*, 2013a). In addition, the JA-responsive

bHLH transcription factors TSAR1 and TSAR2 were shown to regulate the transcriptional activation of specific branches of the *M. truncatula* triterpene saponin biosynthetic pathway (Mertens *et al.*, 2016a; Mertens *et al.*, 2016b).

In this study, we report the identification of Emission of Methyl Anthranilate (EMA) 1, an R2-R3 MYB transcription factor that stimulates the emission of the VOC methyl anthranilate from *M. truncatula* hairy roots.

RESULTS

The R2R3-MYB transcription factor EMA1 is transcriptionally induced in methyl JA-treated *M. truncatula* cells

Triterpene saponin biosynthesis is inducible by methyl JA (MeJA) in suspension-cultured *M. truncatula* cells (Suzuki *et al.*, 2002; Broeckling *et al.*, 2005; Suzuki *et al.*, 2005). To identify additional regulators of triterpene saponin biosynthesis, we further mined our previously reported transcriptome data set of MeJA-treated *M. truncatula* cells (Pollier *et al.*, 2013a). Like *MKB1* (gene tag Mt067 in Figure 1a), transcript levels of gene tag Mt061, corresponding to the *M. truncatula* MYB transcription factor encoded by *Medtr1g086530*, were increased within 30 min of MeJA treatment (Figure 1a). The early MeJA response of *Medtr1g086530* in suspension-cultured *M. truncatula* cells was confirmed by qPCR (Figure 1b) and by probing the *M. truncatula* Gene Expression Atlas (MtGEA; <http://mtgea.noble.org/v3/>; (He *et al.*, 2009)), which includes data from MeJA-treated cell cultures (Figure 1c). We designated the *Medtr1g086530* gene as *Emission of Methyl Anthranilate (EMA) 1*, based on our findings reported here (see further below).

The full-length *EMA1* gene encodes a protein of 278 amino acids with an R2R3-MYB DNA binding domain containing the characteristic regularly spaced tryptophan residues (Figure S1a) that form the hydrophobic core of the helix-turn-helix structure (Saikumar *et al.*, 1990; Dubos *et al.*, 2010). In addition, the EMA1 protein contains a WxPRL motif (Figure S1a), characteristic of the subgroup 20 R2R3-MYB proteins (Kranz *et al.*, 1998; Stracke *et al.*, 2001). A phylogenetic analysis including *Arabidopsis* R2R3-MYB proteins placed EMA1 in subgroup 20 of the R2R3-MYB transcription factor family (Figure S1b), which in *Arabidopsis* consists of six members and is closely related to subgroup 19 that contains three proteins (Dubos *et al.*, 2010). Several R2R3-MYB proteins from both subgroups have been shown to be JA-responsive transcription factors involved in plant developmental processes and stress responses (Cheng *et al.*, 2009; Mandaokar and Browse, 2009; Dubos *et al.*, 2010; Song *et al.*, 2011).

M. truncatula hairy roots overexpressing *EMA1* have a fruity scent

To investigate the potential role of EMA1 as a regulator of triterpene saponin biosynthesis, transgenic *M. truncatula* hairy roots constitutively overexpressing the *EMA1* full-length open reading frame (*EMA1*^{OE}) were generated and overexpression of *EMA1* was confirmed by qPCR (Figure 2a). Strikingly, while handling the hairy roots, we noticed that, in contrast to any of the control lines, the *EMA1*^{OE} lines emitted a fruity aroma. To identify the metabolites responsible for this aroma, the volatiles emitted from control and *EMA1*^{OE} hairy roots were analyzed by gas chromatography – mass spectrometry (GC-MS). This revealed that the *EMA1*^{OE} hairy roots emitted large quantities of the volatile aromatic compound methyl anthranilate (Figure 2b,c), which has a smell similar to the *EMA1*^{OE} lines. Quantitative monitoring of methyl anthranilate production over time showed that the *EMA1*^{OE} hairy roots emitted up to 1,500 ng of methyl anthranilate per h per g of roots, which is about 50 times more than the amount of methyl anthranilate emitted by control roots (Figure 2d). These observations suggest a regulatory role of EMA1 in a process that leads to the emission of methyl anthranilate from *M. truncatula* hairy roots.

To assess whether the overexpression of *EMAI* has a broader impact on the *M. truncatula* metabolome in addition to the induced emission of methyl anthranilate, untargeted metabolite profiling by liquid chromatography electrospray ionization Fourier transform ion cyclotron resonance mass spectrometry (LC-ESI-FT-ICR-MS) was carried out (Pollier *et al.*, 2011). This technique allows profiling metabolites of medium polarity, including saponins and phenolics such as (iso)flavonoids and oligolignols. Peak integration and alignment yielded a total of 10,428 *m/z* peaks. A principal component analysis (PCA) carried out using all *m/z* peaks indicated that the extracts of the EMA1^{OE} hairy roots were clearly different from those of control hairy roots (Figure 2e). To identify the peaks responsible for the observed differences, a supervised partial least squares discriminant analysis (PLS-DA) model separating the EMA1^{OE} and control hairy roots was created and used to generate an S-plot of the correlation and covariance of all *m/z* peaks. Peaks with an absolute covariance value above 0.03 and an absolute correlation value above 0.6 were considered as significantly different. As such, only metabolites with a higher abundance in the EMA1^{OE} lines contributed to the variation between the control and the EMA1^{OE} lines (Figure 2f). The corresponding metabolites were elucidated based on their MSⁿ spectra, thereby revealing that, in addition to the emission of methyl anthranilate, overexpression of *EMAI* leads to higher levels of specific isoflavonoids such as formononetin glucoside malate (FGM) and medicarpin glucoside malate (MGM) (Figure S2, Data S1) in *M. truncatula* hairy roots.

RNA-Seq analysis of the fragrant roots

To assess the mechanism leading to the emission of methyl anthranilate, we performed a genome-wide transcript profiling using RNA-Seq, in which EMA1^{OE} hairy roots were compared to control hairy roots. Illumina HiSeq2000 RNA-Seq was carried out on three independent EMA1^{OE} and control lines, delivering a total of 59.7 million 101-bp paired-end reads. After adapter and quality trimming, the reads were mapped on the *M. truncatula* genome v4.0 (Tang *et al.*, 2014) and counted. Differential expression analysis using the Cuffdiff program of the Cufflinks software package (Trapnell *et al.*, 2010) revealed that the expression of 1,064 of the 41,724 expressed genes was significantly altered in the EMA1^{OE} lines (Table S1). The gene with the highest expression fold-change was *EMAI* itself (Table S1, Figure S3a), confirming overexpression of this MYB transcription factor in the roots analyzed with RNA-Seq.

To identify the genes that are likely the most relevant for the emission of methyl anthranilate from the 1,064 genes with significantly altered expression, a second selection criterion was applied that allowed to compensate for potential biological variation between different *M. truncatula* hairy root lines. Together with the EMA1^{OE} lines, an additional nine *M. truncatula* hairy root lines, that were available from other unrelated research lines and that were transformed with constructs modulating expression of other genes, were therefore subjected to RNA-Seq transcript profiling. These hairy root lines were MKB1^{KD} lines (Pollier *et al.*, 2013a) and hairy roots overexpressing *M. truncatula* orthologs of the Taximin peptide (Onrubia *et al.*, 2014; Colling *et al.*, 2015), none of which emitted a fruity aroma. The Cuffdiff program of the Cufflinks software package (Trapnell *et al.*, 2010) was used to identify genes with significantly altered expression specifically in the EMA1^{OE} lines as compared to the abovementioned other 12 “reference” lines, resulting in a comprehensive list of 68 genes (Table S2), containing only seven genes with an increased expression in the EMA1^{OE} lines as compared to the reference lines, including *EMAI* itself (Table 1, Table S2). Among these seven genes was *Medtr4g018820*, a gene annotated as encoding a JA *O*-methyltransferase, for which higher transcript levels were confirmed by qPCR in EMA1^{OE} hairy roots (Figure S3b,c). Analysis of the predicted protein containing 359 amino acids revealed that *Medtr4g018820* belongs to the *S*-adenosyl-L-methionine (SAM)-dependent carboxyl methyltransferase family

of enzymes, which in turn belong to the larger family of SABATH methyltransferases and act on a variety of substrates, including jasmonic acid, salicylic acid, and anthranilic acid.

As indicated above, besides the emission of methyl anthranilate, we also observed increased amounts of specific isoflavonoids in the EMA1^{OE} lines. However, the expression of none of the hitherto characterized (iso)flavonoid biosynthesis genes was significantly increased in the EMA1^{OE} lines (Table S3), suggesting that the increased accumulation of (iso)flavonoids may be an indirect effect of *EMAI* overexpression. Because of this, we primarily focused on the SAM-dependent carboxyl methyltransferase Medtr4g018820 for further analysis.

***Medtr4g018820* encodes a functional anthranilic acid methyltransferase, MtAAMT1**

To functionally characterize Medtr4g018820 and to assess its plausible role in the accumulation of methyl anthranilate, we first constructed a phylogenetic tree using a set of biochemically characterized SAM-dependent carboxyl methyltransferases (SMTs) involved in the methylation of small acids. The Medtr4g018820 protein clustered together with the salicylic acid methyltransferases, all of which could also methylate benzoic acid to a lesser extent (Figure 3a) (Ross *et al.*, 1999; Negre *et al.*, 2002; Pott *et al.*, 2004; Tieman *et al.*, 2010; Zhao *et al.*, 2013). This cluster also contains the benzoic acid methyltransferase from *Nicotiana suaveolens* that can additionally methylate salicylic acid (Pott *et al.*, 2004). Notably, the closely related salicylic acid methyltransferase from *Glycine max* was also shown to be capable of catalyzing the methylation of anthranilic acid in addition to salicylic acid and benzoic acid (Lin *et al.*, 2013). Second, a sequence clustering analysis performed with the functionally characterized SMTs indicated the conserved SAM-binding residues in Medtr4g018820 (Figure S4). The well-conserved motif I includes the GxGxG consensus, in which none of the three glycine residues are universally conserved, but are replaced by residues with small side chains, and is considered the hallmark SAM-binding site of the SMTs (Kozbial and Mushegian, 2005). In our clustering analysis, Medtr4g018820 and all the plant-specific SMTs involved in the methylation of small acids contained the conserved GxSxG consensus in motif I. In addition to the not so well defined motifs II and III, a very well conserved, yet undescribed, motif defined by the consensus (F/L)xDLPxNDFN was also identified between motifs I and II in all the aligned SMTs (Figure S4). Hence, *Medtr4g018820* likely encodes a protein involved in the methylation of small acids.

To identify the substrate(s) of Medtr4g018820, we expressed the full-length gene in *Escherichia coli* and fed the induced *E. coli* cultures with five different small acid substrates including anthranilic acid, benzoic acid, *p*-coumaric acid, jasmonic acid and salicylic acid to a final concentration of 1 mM. Organic extracts of the *E. coli* cultures were analyzed by GC-MS and compared to authentic methylated standards, which confirmed the *O*-methylation of all substrates, except *p*-coumaric acid. To determine the relative activity of Medtr4g018820 with each substrate, we purified a HIS-tagged version of the protein for *in vitro* assays. The purified protein was combined with 1 mM of the substrate and ¹⁴C radiolabeled SAM for 40 min, after which organic extracts of the reaction mixture were used to determine counts per minute (cpm) values using a liquid scintillation counter. The highest cpm value and therefore methylation activity was observed for anthranilic acid, followed by benzoic acid, salicylic acid and jasmonic acid (Figure 3b). Finally, we determined the kinetic properties of the purified protein for the methylation of anthranilic acid and benzoic acid, the two substrates for which most methylation was observed. The protein has a K_m value of 424.2 μM and a k_{cat} value of 77.4 s^{-1} ($k_{cat}/K_m = 182.4 \text{ s}^{-1}\text{mM}^{-1}$) for anthranilic acid as a substrate. Similarly, for benzoic acid, the protein possesses a K_m value of 659.8 μM and a k_{cat} value of 4.5 s^{-1} ($k_{cat}/K_m = 6.8 \text{ s}^{-1}\text{mM}^{-1}$) (Figure 3c). Because the kinetic efficiency (k_{cat}/K_m value) of Medtr4g018820 for methylation of anthranilic acid was the highest, the enzyme was named *M. truncatula* anthranilic acid methyltransferase 1 (MtAAMT1).

Anthranilic acid is an intermediate of the tryptophan biosynthesis pathway and is synthesized directly from chorismate, which itself is the end-product of the shikimate pathway and which is also the precursor for the synthesis of the aromatic amino acids phenylalanine and tyrosine. If expression of *EMA1* affected the expression of genes encoding methyl anthranilate biosynthesis enzymes in addition to *MtAAMT1*, transcriptional effects may for instance be visible on the genes encoding anthranilate synthase. Anthranilate synthase catalyzes the first step of the tryptophan biosynthesis pathway by converting chorismate into anthranilic acid and consists of two non-identical subunits, anthranilate synthase α (ASA) and anthranilate synthase β (ASB). Arabidopsis encodes two characterized ASA enzymes (Niyogi and Fink, 1992), ASA1 (AT5G05730) and ASA2 (AT2G29690). A BlastP search in the *M. truncatula* genome v4.0 with ASA1 as query revealed four ASA orthologues, Medtr1g114520, Medtr3g070290, Medtr3g076770, and Medtr3g467000. The expression of these four orthologues was probed for in the RNA-Seq data of the EMA1^{OE} lines. *Medtr3g076770* and *Medtr3g467000* turned out not to be expressed in hairy roots (FPKM = 0), whereas the expression of *Medtr1g114520* and *Medtr3g070290* was similar in the CTR and EMA1^{OE} lines (Figure S5). Arabidopsis encodes one ASB enzyme (Niyogi *et al.*, 1993), AT1G25220, for which an ortholog (Medtr1g033480) was encountered in the *M. truncatula* genome (v4.0). Its expression was slightly (1.39-fold), but not significantly (q-value = 0.078) enhanced in the EMA1^{OE} lines (Figure S5). Thus, the effect of overexpression of *EMA1* on methyl anthranilate biosynthesis seems to be restricted to *MtAAMT1*.

The transcriptional activator EMA1 does not transactivate the *MtAAMT1* promoter

Because overexpression of *EMA1* in *M. truncatula* hairy roots leads to the emission of methyl anthranilate, we postulated that EMA1 would act as a direct transcriptional activator of the *MtAAMT1* promoter. To test this hypothesis, we first assessed the potential transactivation activity of EMA1 using transient expression assays in tobacco protoplasts (De Sutter *et al.*, 2005; Vanden Bossche *et al.*, 2013). EMA1 was fused in-frame to the GAL4 DNA-binding domain and co-expressed in tobacco protoplasts with the firefly luciferase reporter gene (*fLUC*) under the control of the *UAS* promoter that contains a tandem repeat of five GAL4 binding elements. Compared to the fLUC activity in the control, targeting of EMA1 to the *UAS* promoter led to a 40-fold increase in fLUC activity in tobacco protoplasts (Figure 4a), indicating that EMA1 can act as a transcriptional activator.

Next, we assessed if EMA1 could activate the *MtAAMT1* promoter in tobacco protoplasts. To this end, the 1000-bp region immediately upstream of the *MtAAMT1* start codon was cloned in front of the *fLUC* reporter gene. When this promoter construct was co-transfected in tobacco protoplasts with EMA1 driven by the cauliflower mosaic virus 35S promoter (pCaMV35S), no relevant increase in fLUC activity was observed (Figure 4b). To ensure that this was not a result of the lack of regulatory elements that may be located more distally from the transcription initiation site, the 2000-bp region immediately upstream of the *MtAAMT1* start codon was cloned in front of the *fLUC* reporter gene. Again, no relevant increase in fLUC activity was observed when this promoter construct was co-transfected in tobacco protoplasts with EMA1 driven by the CaMV35S promoter (Figure 4b), indicating that EMA1 could not transactivate the *MtAAMT1* promoter in tobacco protoplasts.

EMA1 transactivates the *MtPLATZ1* promoter

As EMA1 does not directly activate the *MtAAMT1* promoter, we screened the list of genes with significantly altered expression identified through the RNA-Seq analysis (Table 1) for transcription factors that could be involved in the signaling that results in the activation of the *MtAAMT1* promoter. Among the seven genes with a higher expression level in the EMA1^{OE} lines was another transcription factor, *Medtr4g094680*. This gene corresponds to a putative

Plant AT-rich sequence and Zinc-binding (PLATZ) transcription factor, which we named *MtPLATZ1* for *M. truncatula* PLATZ transcription factor 1. The higher occurrence of *MtPLATZ1* transcripts in the EMA1^{OE} hairy roots was confirmed by qPCR (Figure 4c). Furthermore, when the 1000-bp *MtPLATZ1* promoter was co-transfected with EMA1 driven by the CaMV35S promoter in tobacco protoplasts, a 9-fold increase in the fLUC activity was observed as compared to the fLUC activity in protoplasts co-transfected with a GUS control (Figure 4d). Hence, *MtPLATZ1* can be considered a direct target of EMA1.

Analysis of the 1000-bp *MtPLATZ1* promoter in the PlantCARE database (Lescot *et al.*, 2002) revealed the presence of a triple repeat of the MYB recognition element (MRE) AACCTAA, 157-174 bp upstream of the start-codon (Figure S6a). Because EMA1 is a MYB transcription factor, we reasoned that this 17-bp domain may be essential for binding of EMA1 to the *MtPLATZ1* promoter and its subsequent transcriptional activation. To substantiate this hypothesis, we first cloned two versions of the *MtPLATZ1* promoter: a promoter construct containing the 198 bp upstream of the *MtPLATZ1* start codon that contains the MRE repeats (+MRE) and a promoter construct containing the 149 bp upstream of the *MtPLATZ1* start codon, in which the MRE repeats are not present (-MRE; Figure S6a). Transactivation assays in tobacco protoplasts using the +MRE and -MRE *MtPLATZ1* promoter constructs revealed that the MRE repeats-containing region between 149 and 198 bp is essential for the activation of the *MtPLATZ1* promoter by EMA1 (Figure 4e). Next, we mutated the 17-bp domain containing the triple MRE repeat in the 1000-bp *MtPLATZ1* promoter (Figure S6b) and compared the activation of this promoter by EMA1 with the activation of the wild-type promoter in tobacco protoplast assays. Confirming our previous experiments, the wild-type 1000-bp *MtPLATZ1* promoter was activated when EMA1 was co-transfected, whereas this activation was absent when the 1000-bp mutated *MtPLATZ1* promoter was used (Figure 4f). From these protoplast assays, it can be concluded that the 17-bp domain containing the MRE repeats in the *MtPLATZ1* promoter is essential for its transactivation by EMA1. Scanning of the 2-kb upstream region of the *MtAAMT1* gene revealed the absence of MRE motifs, which is in agreement with the observed lack of transactivation in the protoplast assays.

EMA1 binds the *MtPLATZ1* promoter through a repeated ACCTAAC motif

To prove that EMA1 directly binds the MRE sequence of the *MtPLATZ1* promoter, two additional experiments were carried out. First, binding of EMA1 to the *MtPLATZ1* promoter was investigated by yeast one-hybrid (Y1H) analysis (Deplancke *et al.*, 2004). To this end, we made three different promoter constructs (Figure S6c). The first construct contained the nucleotide sequence of the wild-type *MtPLATZ1* promoter between 214 and 117 bp upstream of the start-codon, which includes the 17-bp domain containing the MRE repeats. The second construct contained the same promoter sequence, but with the 17-bp domain mutated. Finally, a synthetic construct was made that contains a triple repeat of the 17-bp domain. Upon transformation with EMA1, growth on 3-amino-1,2,4-triazole (3-AT)-containing medium was observed for *EMA1*-expressing yeast containing the wild-type *MtPLATZ1* promoter fragment, whereas no growth was observed for *EMA1*-expressing yeast containing the mutated *MtPLATZ1* promoter fragment (Figure 5a). In addition, *EMA1*-expressing yeast containing the synthetic construct with the triple repeat of the 17-bp domain grew markedly better than yeast containing the wild-type promoter sequence (Figure 5a). Hence, the Y1H analysis indicated that EMA1 directly binds the 17-bp MRE repeat containing domain of the *MtPLATZ1* promoter.

To further evidence this, we characterized the target sequence of EMA1 using a protein-binding microarray that contains all possible double-stranded 11-mers (Godoy *et al.*, 2011). To this end, recombinant N-terminal maltose binding protein (MBP)-tagged EMA1 was produced in *E. coli* and used to hybridize to the protein-binding microarray. This analysis revealed that EMA1 recognizes the MYB binding site IIg (MBSIIg) consensus sequence (GKTWGGTR;

where R = A or G; K = G or T; W = A or T; (Franco-Zorrilla *et al.*, 2014)) with very high affinity. The top-scoring sequence motif GTTAGGT (Figure 5b) is the reverse complement of ACCTAAC, a sequence motif that is repeated thrice in the 17-bp sequence domain (Figure S6a) that was shown to be essential for binding of EMA1 (Figure 4e,f and Figure 5a). When all high-affinity 8-mer sequences (E-score ≥ 0.45) are listed, all but one of them correspond to a MBSIIg motif (Table S4). Similarly, the E-score distributions of several MBS sequences again pointed towards MBSIIg as being the preferred binding site of EMA1 (Figure 5c). Taken together, these data indicate that EMA1 binds to the *MtPLATZ1* promoter through a promoter domain containing a repeated ACCTAAC sequence. Notably, though this consensus sequence could not be detected in the upstream region of the *MtAAMT1* gene, a perfect match could be detected in the proximal upstream region of the coding sequences of the genes *Medtr6g059650* and *Medtr2g090245*, which are among the most highly upregulated genes besides *MtAAMT1* in the EMA1^{OE} lines (Table 1).

Overexpression of the transcriptional repressor MtPLATZ1 in *M. truncatula* hairy roots leads to repression of *EMA1* and *MtAAMT1* expression

PLATZ proteins are plant-specific zinc-dependent DNA-binding proteins that were reported to function as transcriptional repressors by binding AT-rich promoter sequences (Nagano *et al.*, 2001). Structural analysis of the MtPLATZ1 protein revealed the presence of the two conserved PLATZ domains as identified by Nagano *et al.* (2001) (Figure S7). To assess its potential repressor activity, MtPLATZ1 was fused in-frame to the GAL4 DNA-binding domain and co-expressed in tobacco protoplasts with the *fLUC* reporter gene under the control of the *UAS* promoter. Compared to the fLUC activity in the control, targeting of MtPLATZ1 to the *UAS* promoter led to a significant 7-fold decrease in the fLUC activity (Figure 6a), indicating that MtPLATZ1 can act as a transcriptional repressor.

To assess the role of MtPLATZ1 in the signaling cascade leading to the transcriptional activation of *MtAAMT1* upon ectopic expression of *EMA1*, hairy roots overexpressing *MtPLATZ1* were generated and overexpression of *MtPLATZ1* was confirmed by qPCR (Figure 6b). Unlike the EMA1^{OE} lines, the MtPLATZ1^{OE} roots were not fragrant when cultured on solid medium. Hence, overexpression of *MtPLATZ1* does not lead to the emission of methyl anthranilate. Surprisingly, we noticed a nearly 10-fold reduction in the expression of *EMA1* in the MtPLATZ1^{OE} lines as compared to the control lines (Figure 6c). Because high expression of *EMA1* is required for emission of methyl anthranilate from *M. truncatula* hairy roots, the transcriptional silencing of *EMA1* could explain the lack of methyl anthranilate emission from these lines. Indeed, when probed for by qPCR, also the expression of *MtAAMT1* was slightly decreased in the MtPLATZ1^{OE} lines as compared to the control lines (Figure 6d). This observation supports a role of EMA1 as a positive regulator of *MtAAMT1*, however, the transcriptional repression of *MtAAMT1* seems less pronounced compared to the repression of *EMA1*, implying that EMA1 may not be the only factor involved in the regulation of *MtAAMT1* expression. To assess whether MtPLATZ1 can directly repress, transactivation assays in tobacco protoplasts with the *MtAAMT1* promoter and MtPLATZ1 were carried out. No relevant decrease in fLUC activity was observed (Figure 6e), indicating that MtPLATZ1 could not repress the *MtAAMT1* promoter in tobacco protoplasts.

Methyl anthranilate treatment leads to induction of *EMA1*, *MtAAMT1* and *MtPLATZ1* expression

To get some insight into the possible biological roles of *in planta* methyl anthranilate production in *M. truncatula*, we carried out expression analysis in two stages. First, we mined the MtGEA for differential expression of *EMA1*. Besides the abovementioned induction of *EMA1* expression in MeJA-treated cell cultures (Figure 1c), this revealed a strong induction of *EMA1*

expression in *M. truncatula* cell cultures treated with yeast elicitor (YE) and in the roots of *M. truncatula* seedlings treated with NaCl (Figure S8). Notably, this analysis also further corroborated that none of the transcripts corresponding to the *M. truncatula* *ASA* and *ASB* genes were induced in the condition in which *EMA1* transcript levels increased (Figure S8).

Although the data available on the MtGEA were limited, they nonetheless suggested a possible link between the induction of *EMA1*, and thus possibly the activation of methyl anthranilate, and biotic and/or abiotic stress responses. To further assess this, we launched a set of experiments in which we treated *M. truncatula* hairy root cultures with a number of (a)biotic stress agents and probed the expression of *EMA1*, *MtAAMT1*, and *MtPLATZI*. This analysis confirmed the induction of *EMA1* expression in response to MeJA, YE and NaCl, although it was not as strong as in the experiments reported on the MtGEA, namely ca. four- to six-fold (Figure S9a). Additionally, we also probed the effect of salicylic acid and flagellin. The effect of salicylic acid was comparable to that of MeJA, YE and NaCl but the effect of flagellin was more pronounced, leading to a ca. 20-fold induction of *EMA1* expression after 2 hours of treatment (Figure S9a). Together, these observations further support a link between induction of *EMA1* expression and response to (a)biotic stresses. Notably, also *MtAAMT1* expression was moderately, but significantly induced after flagellin treatment, further supporting the correlation between *EMA1* and *MtAAMT1* expression (Figure S9b). No significant effects on *MtPLATZI* transcript levels in any of the stress conditions were observed (Figure S9c).

Finally, we also assessed the effect of methyl anthranilate on the expression of the three genes. This revealed a surprisingly strong effect on *EMA1* transcript levels, which were increased several thousand-fold after 24 hours of methyl anthranilate treatment (Figure 6f). In agreement with the proposed regulatory role of *EMA1* in the regulation of *MtAAMT1* and *MtPLATZI*, transcript levels of these two genes were respectively increased by more than 100- and thousand-fold as well after 24 hours of methyl anthranilate treatment (Figure 6g-h). This may suggest that the regulation of methyl anthranilate biosynthesis by *EMA1* is subject to a positive feedback loop.

DISCUSSION

In our discovery program to elucidate the regulation of specialized metabolism in *M. truncatula*, we identified the R2-R3 MYB transcription factor *EMA1* that, upon ectopic expression in *M. truncatula* hairy roots, leads to the emission of methyl anthranilate, giving the transgenic roots a pleasant odor. Transcript profiling of the *EMA1*-overexpressing hairy roots using RNA-Seq revealed that the SAM-dependent carboxyl methyltransferase-encoding gene *MtAAMT1* was expressed higher in the fragrant roots. Through *in vitro* assays with recombinant *MtAAMT1* and different small acid substrates, we confirmed that this protein efficiently converts anthranilic acid to methyl anthranilate. In plants, convergent evolution gave rise to two separate mechanisms for the synthesis of methyl esters, and both mechanism have been demonstrated to lead to methyl anthranilate synthesis (Pichersky and Lewinsohn, 2011). The first methyl anthranilate synthesis mechanism involves a member of the BAHD family of acyltransferases and was thus far reported only in Washington Concord grape (*Vitis labrusca*) in which anthraniloyl-coenzyme A (CoA):methanol acyltransferase (AMAT) catalyzes the formation of methyl anthranilate from anthraniloyl-coenzyme A (CoA) and methanol (Wang and De Luca, 2005). The second mechanism was demonstrated first in maize, where a member of the SABATH family of methyltransferases catalyzes the transfer of a methyl group from *S*-adenosyl-L-methionine to anthranilic acid (Köllner *et al.*, 2010). A phylogenetic analysis indicated that the SAM-dependent *MtAAMT1* belongs to the SABATH family of methyltransferases (Figure 3a), which also includes the strawberry (*Fragaria x ananassa*) *FanAAMT* that catalyzes methyl anthranilate synthesis in cultivated strawberry (Pillet *et al.*, 2017).

We demonstrated that EMA1 binds and transactivates gene expression through the MRE cis-element, but no MRE motifs could be found in the 5' upstream region of the *MtAAMT1* gene (corresponding to the intergenic region till *Medtr4g018830*). This could explain why we were unable to unambiguously establish that EMA1 is a direct regulator of *MtAAMT1* expression by means of the transactivation assays with *MtAAMT1* promoter sequences. Notably however, intron 1 of the *MtAAMT1* gene contains the sequence CACCTAAT, which is a near perfect match to the reverse complement of the consensus sequence GKTWGGTR identified through the protein-binding microarray analysis as the preferred EMA1 motif. Alternatively, it cannot be excluded that a more complex transcriptional network, involving other, yet unknown transcriptional regulators or other regulatory elements, is necessary for the onset of *MtAAMT1* expression in EMA1^{OE} hairy roots. In our tentative regulatory model (Figure 7), we provide a few possible scenarios for the mode of action of EMA1 in the activation of *MtAAMT1* expression. EMA1 might indirectly activate transcription of *MtAAMT1* through interaction with a yet unknown transcription factor or modulate *MtAAMT1* expression indirectly by activating transcription of a yet unknown direct regulator of *MtAAMT1*. On the other hand, in addition to *MtAAMT1*, the transcription factor-encoding gene *MtPLATZ1* appeared within the set of genes upregulated in the fragrant roots. The *MtPLATZ1* promoter does indeed contain the MRE motifs and we could establish *MtPLATZ1* as a direct EMA1 target. Conversely however, ectopic expression of *MtPLATZ1* in *M. truncatula* hairy roots leads to the transcriptional silencing of *MtAAMT1*, thereby excluding that *MtPLATZ1* would relay a positive regulatory signal through EMA1 to activate *MtAAMT1* expression but simultaneously revealing an additional layer of complexity to the regulation of the emission of methyl anthranilate from *M. truncatula* hairy roots, namely the existence of a negative transcriptional feedback loop involving the *M. truncatula* *MtPLATZ1* protein.

Here, we demonstrated *MtPLATZ1* to be a transcriptional repressor protein in a complex transcriptional network that controls the emission of VOCs from *M. truncatula* (hairy) roots. Apart from their initial discovery as transcriptional repressors almost two decades ago (Nagano *et al.*, 2001), no studies have been published on plant PLATZ proteins until very recently, with four new studies shedding light on the possible functions of this enigmatic family of transcription factors (Li *et al.*, 2017a; Kim *et al.*, 2018; Wang *et al.*, 2018; Zhang *et al.*, 2018). Originally, the pea (*Pisum sativum*) PLATZ1 protein was shown to non-specifically bind to A/T-rich sequences in the upstream regions of pea genes and mediate transcriptional repression (Nagano *et al.*, 2001). More recently however, the maize (*Zea mays*) *floury3* (*FL3*) gene was found to encode a PLATZ protein that can physically interact with two critical factors of the RNA polymerase III (RNAPIII) transcription complex, namely RNA polymerase III subunit 53 (RPC53) and transcription factor class C 1 (TFC1). Thereby FL3 can modulate the function of RNAPIII in transcribing tRNAs and 5S rRNA (Li *et al.*, 2017a). Subsequent analysis revealed the phylogeny of the PLATZ family in maize and indicated that all maize PLATZ proteins locate to the nucleus, consistent with their predicted role as transcription factors and that some of them interacted with both RPC53 and TFC1, some with either RPC53 or TFC1, whereas others had no protein-protein interaction with these two factors. Together, these findings further support that maize PLATZ proteins may be generally involved in the modulation of RNAPIII-mediated small non-coding RNA transcription (Wang *et al.*, 2018). Through this action, they may modulate endosperm development and storage reserve filling in maize seeds (Wang *et al.*, 2018), leaf growth and senescence in Arabidopsis (Kim *et al.*, 2018), or responses to abiotic stresses in cotton (*Gossypium hirsutum*) and Arabidopsis (Zhang *et al.*, 2018).

In addition to the (indirect) transcriptional silencing of *MtAAMT1*, *MtPLATZ1* also represses the expression of *EMA1*; we postulate either by direct binding of the *EMA1* promoter or through activation of the expression of a repressing ncRNA, given our own findings or the

recently reported roles of PLATZ proteins (Figure 7). As such, it seems that EMA1 directly activates a regulatory feedback loop that leads to its own repression. Such a regulatory feedback loop has been observed for other processes involved in plant specialized metabolism. For instance, binding of the jasmonate hormone to its receptor SCF^{COI1} will lead to proteasomal degradation of the JAZ repressor proteins, thereby liberating MYC2 that is responsible for the transcriptional activation of the jasmonate-mediated defense responses that include the production of bioactive specialized metabolites. However, MYC2 will also directly bind and activate the promoters of the JAZ repressor proteins, which in turn will lead to the repression of MYC2 and revert the cellular machinery to its original state (Chini *et al.*, 2007; Pauwels and Goossens, 2011; Wasternack and Hause, 2013). Similarly, the R2R3-MYB transcription factor EOBI that regulates the production of VOCs in petunia flowers also activates the expression of *ODO1*, which, in turn, negatively affects *EOBI* expression (Spitzer-Rimon *et al.*, 2012). Hence, it seems that the existence of such negative feedback loops is widespread in plant specialized metabolism to guarantee appropriate and timely production of particular volatiles or other bioactive specialized metabolites and, conversely, safeguard development by shielding the plant from unnecessary or inappropriate overaccumulation of such metabolites. In case of methyl anthranilate, such complex regulatory loops make ecological sense since this volatile has been reported to have diverse effects, pending on the concentration and location of production. Indeed, in some plant species, such as apple, concord grape, and strawberry, methyl anthranilate attributes odor to the fruits, which serves as an attractant for beneficial insects and simultaneously perhaps also as a pathogen defense compound (Robacker *et al.*, 2011; Chambers *et al.*, 2013). Conversely, in maize organs, methyl anthranilate has reported repellent effects against insect larvae and birds (Esther *et al.*, 2013; Bernklau *et al.*, 2016). The role of methyl anthranilate is still under debate. The above cited literature suggests a role in interaction with the environment. This appears to be sustained by our observation that *EMA1* expression in *M. truncatula* organs is induced by biotic and abiotic stress agents, such as flagellin, yeast elicitor and salt. Finally, we have also revealed the existence of a potential amplification loop, as supported by our observation that methyl anthranilate can boost expression of both *EMA1* and *MtAAMT1*. As such, the tentative regulatory model that we propose for the biosynthesis of methyl anthranilate (Figure 7) becomes very reminiscent of that of the JAs, which is heavily loaded with amplification and feedback loops (Pauwels *et al.*, 2009; Wasternack and Hause, 2013). Although it becomes tentative to speculate about methyl anthranilate as a molecule with potential hormonal-like signaling roles in plants, this requires more profound investigation.

EXPERIMENTAL PROCEDURES

Generation and cultivation of *M. truncatula* suspension cell cultures and transformed *M. truncatula* hairy root cultures

Maintenance and MeJA elicitation of *M. truncatula* suspension cell cultures were carried out as described (Pollier *et al.*, 2013a). *M. truncatula* (ecotype Jemalong J5) hairy roots were generated via *A. rhizogenes*-mediated transformation and maintained as described (Pollier *et al.*, 2011).

Sequence alignment and phylogenetic analysis

The protein sequences of the *Arabidopsis* MYB transcription factors and the functionally characterized small acid methyltransferases were retrieved from GenBank (<http://www.ncbi.nlm.nih.gov/genbank/>) and aligned with ClustalW. The phylogenetic tree was generated with MEGA 5.10 software (Tamura *et al.*, 2011), according to the Neighbor-Joining method and bootstrapping with 1,000 replicates. The evolutionary distances were computed with the Jones-Taylor-Thornton (JTT) model and all positions containing gaps and missing data were eliminated from the data set using the complete deletion option.

Generation of DNA constructs

The *EMAI*, *MtAAMT1* and *MtPLATZ1* full-length open reading frames were PCR-amplified (for primer sequences, see Table S5) from *M. truncatula* (ecotype Jemalong J5) cDNA, cloned into the donor vector pDONR207 by Gateway recombination and sequence-verified. The promoter regions of *EMAI*, *MtAAMT1* and *MtPLATZ1* were determined using the *M. truncatula* genome v4.0 (Tang *et al.*, 2014), PCR-amplified (for primer sequences, see Table S5) from *M. truncatula* (ecotype Jemalong J5) genomic DNA, cloned into the donor vector pDONR207 by Gateway recombination and sequence-verified.

For stable overexpression in *M. truncatula* hairy roots, the entry clones were Gateway-recombined into the pK7WG2D binary vector (Karimi *et al.*, 2002) and the resulting expression clones were transformed into the *Agrobacterium rhizogenes* strain LBA 9402/12 for generation of hairy roots. For expression in *E. coli* BL21(DE3) and inducible protein production, the *MtAAMT1* gene was Gateway-recombined into the destination vector pDESTTM17 (Invitrogen, Carlsbad, CA, USA) containing the N-terminal 6x HIS tag. For protoplast assays, the transcription factors and promoters were Gateway-recombined into the p2GW7 and pGWL7 vectors, respectively (Vanden Bossche *et al.*, 2013).

Quantitative PCR (qPCR) gene expression analysis

For qPCR analysis, total RNA was extracted from *M. truncatula* tissues using the RNeasy mini kit (Qiagen, Hilden, Germany). cDNA was prepared using the iScriptTM cDNA Synthesis Kit (Bio-Rad, Hercules, CA, USA). Primer design and qPCR analysis were carried out as described (Pollier *et al.*, 2013a). All primers used for this study are listed in Table S5.

Metabolite profiling

The volatiles emitted from the *M. truncatula* hairy roots were profiled as described (Boachon *et al.*, 2015) with modifications. Briefly, hairy roots grown on solid medium (Pollier *et al.*, 2011) were placed in sealed 1-L glass jars equipped with inlet and outlet connectors. The volatiles emitted by the roots were pumped out the jars with a vacuum pump at about 100 mL/min and trapped at the outlet on a cartridge containing 150 mg Tenax TA (20/35 mesh). The incoming air was purified through a similar cartridge. Volatiles were sampled for 6 h and 2 μ L of 400 μ M of nonyl acetate (Sigma-Aldrich) was added to each cartridge as an internal standard. Subsequently, the Tenax cartridges were analyzed on a PerkinElmer Clarus 680 equipped with a Perkin Elmer Clarus 600T quadrupole mass spectrometer and a TurboMatrix 100 thermal desorber (TDS) (PerkinElmer) as previously described (Boachon *et al.*, 2015). Methyl anthranilate was identified on the basis of its retention time and mass spectrum and compared to an authentic standard (Sigma-Aldrich). Quantification of volatile emission was carried out by integration of the specific *m/z* ion peaks 151 and 126 at the retention time of methyl anthranilate and nonyl acetate respectively, and using standard curves established with a concentration range of authentic standards. Emission was calculated as the mass of methyl anthranilate emitted per mass of fresh weight of roots per hour.

For untargeted metabolite profiling, *M. truncatula* hairy roots were harvested and extracted as reported (Pollier *et al.*, 2011), and LC-ESI-FT-ICR-MS analysis was carried out as described (Pollier and Goossens, 2013). Chromatograms were integrated and aligned with the XCMS software package (Smith *et al.*, 2006) in R version 2.6.1 using the following parameter values: *xcmsSet* (*fwhm* = 10, *max* = 300, *snthresh* = 2, *mzdiff* = 0.05), *group* (*bw* = 10, *max* = 300), *rector* (*method* = *loess*, *family* = *symmetric*). A second grouping was carried out with the same parameter values.

For the *E. coli* feeding assay, GC-MS was performed using GC model 6890 and MS model 5973 (Agilent Technologies). A 1- μ L aliquot was injected in splitless mode into a VF-5ms capillary column (Varian CP9013, Agilent Technologies) and operated at a constant helium flow

of 1 mL/min. The injector was set to 280°C and the oven was held at 35°C for 2 min post injection, ramped to 280°C at 10°C/min, held at 280°C for 15 min, and cooled to 35°C at 50°C/min at the end of the run. The MS transfer line was set to 250°C, the MS ion source to 230°C, and the quadrupole to 150°C, throughout. For identification of metabolites, full EI-MS spectra were generated by scanning the m/z range of 60-800.

RNA-Seq analysis

Illumina HiSeq2000 RNA sequencing (100 bp paired-end reads, TruSeq® RNA sample preparation) was carried out for three independent control and EMA1^{OE} lines by the UZ Leuven Genomics Core (<http://gc.uzleuven.be/>). As described (Pollier *et al.*, 2013b) and using default parameters, the raw RNA-Seq reads were quality-trimmed and mapped on the *M. truncatula* genome v4.0 (Tang *et al.*, 2014) with TOPHAT v2.0.3 (Trapnell *et al.*, 2009). Uniquely mapped reads were counted and FPKM values determined with CUFFLINKS version v1.3.0. (Trapnell *et al.*, 2010). Differential expression analyses were performed using the Cuffdiff algorithm of the CUFFLINKS software package (Trapnell *et al.*, 2010).

E. coli substrate feeding and *in vitro* enzyme kinetic assays

One Shot® *BL21(DE3)* chemically competent *E. coli* (Invitrogen) cells transformed with the pDEST17[*T7/MtAAMT1*] vector were used for the *in vivo* substrate feeding assay and for protein purification for the *in vitro* assays. For the substrate feeding assay, an overnight culture was used to inoculate five flasks of 50 mL Luria-Bertani broth to a starting optical density of 0.05. The flasks were incubated at 37°C for 1 h and induced with isopropyl β -D-1-thiogalactopyranoside (IPTG) added to a final concentration of 1 mM. To induce protein production, the cultures were incubated at 20°C for 30 min prior to the addition of anthranilic acid, benzoic acid, *p*-coumaric acid, jasmonic acid or salicylic acid to a concentration of 1 mM, and incubated further for 3 h. All the substrates were dissolved in 50% ethanol to obtain a stock solution of 100 mM, except jasmonic acid, which was dissolved to 1 M. Finally, the cells were collected and extracted with 3 mL of hexane, which was used for GC-MS analysis.

For the *in vitro* assays, MtAAMT1 was purified from a 500-mL culture using Ni-NTA agarose (Qiagen) and the bound protein was eluted with 250 mM imidazole. To determine the relative activity of MtAAMT1 for the methylation of different substrates, a 50- μ L reaction was set up. For this, 10 μ L purified protein (1.67 μ g/ μ L), 10 μ L assay buffer (250 mM Tris-HCl pH 7.5 and 25 mM KCl), 0.5 μ L of 100 mM substrate and 28.5 μ L water were mixed and incubated at 25°C for 5 min. The reaction was initiated by the addition of 1 μ L S-[methyl-¹⁴C]-Adenosyl-L-Methionine (56.3 mCi/mmol, PerkinElmer), incubated for 40 min, and terminated by the addition of 3 μ L of concentrated HCl. The reaction mixture was extracted with 100 μ L of ethylacetate, 30 μ L of which was transferred to a scintillation vial, mixed with 1.5 mL of scintillation fluid (PerkinElmer, Waltham, MA, USA) and counted in a Triathler scintillation counter (Hidex, Turku, Finland). Relative enzyme activity with each substrate was calculated as cpm and the product which reached the highest value was set to 100%.

To determine the kinetic properties of MtAAMT1, the same assay set-up was used with varying concentrations of the substrate ranging from 0 to 2 mM for anthranilic acid and from 0 to 5 mM for benzoic acid. Steady-state kinetic constants V_{max} , K_m and k_{cat} and their errors were determined by fitting the initial velocity versus anthranilic acid or benzoic acid concentrations to the hyperbolic Michaelis-Menten equation using GraphPad Prism version 6. Enzyme concentration used for the assay was calculated using Bradford's colorimetric assay.

Protoplast assays

Transient expression assays in *Nicotiana tabacum* protoplasts were performed as described (De Sutter *et al.*, 2005; Vanden Bossche *et al.*, 2013). Briefly, protoplasts prepared from tobacco

Bright Yellow-2 (BY-2) cells were transfected with three different plasmids. The first plasmid (reporter plasmid) contained the *firefly luciferase (fLUC)* gene under control of the promoter being investigated; the second plasmid (effector plasmid) contained the transcription factor being investigated driven by the CaMV35S promoter and the third plasmid (normalizer plasmid) contained the *Renilla luciferase (rLUC)* gene under control of the pCaMV35S. The transfected protoplasts were incubated overnight and lysed to determine fLUC and rLUC activities using the Dual-Luciferase® Reporter Assay System (Promega, Madison, WI, USA). The fLUC activity is a measure of the activity of the investigated promoter, whereas the rLUC activity reflects the transfection efficiency. For normalization, the fLUC value of each independent transfection was divided by the corresponding rLUC value. For each investigated transcription factor, eight transfections were performed and the normalized fLUC values were averaged and compared relative to the values obtained from transfections with an effector plasmid containing the *GUS* gene.

To assess whether a transcription factor acts as a transcriptional activator or repressor, the protoplast assays were carried out as described above, but with different reporter and effector plasmids. The reporter plasmid contained the *fLUC* gene under control of the *UAS* promoter that contains a tandem repeat of five GAL4 binding elements upstream of a truncated pCaMV35S (Ohta *et al.*, 2000). The effector plasmid contained the investigated transcription factor fused in-frame to the GAL4 DNA-binding domain. To assess activation or repression, normalized and averaged fLUC values were compared to the normalized and averaged fLUC values of an “empty” effector plasmid.

Yeast one-hybrid analysis

Yeast one-hybrid analysis was performed as described (Deplancke *et al.*, 2004). Fragments (97 bp) of the wild-type and mutated *MtPLATZ1* promoter were amplified using primers 3371 and 3372 (Table S5) and recombined into the donor vector pDONRP4-P1R. The 103-bp fragment containing the triple repeat of the MRE-box was generated using the primers 3373-3378. First, double-stranded DNA fragments were generated using primer pairs 3373/3374 and 3375/3376. Subsequently, the two fragments were mixed and used as template for a PCR with primers 3377 and 3378. The resulting fragment was recombined into the donor vector pDONRP4-P1R. Sequence-verified entry clones were recombined with the DNA bait::*HIS3* reporter plasmid pMW#2 and the resulting constructs were linearized using *Afl*III prior to transformation into yeast strain YM4271 (Deplancke *et al.*, 2004). The obtained yeast strains were transformed with EMA1 in the prey vector pDEST22 (Invitrogen) or the empty pDEST22 vector. Transformants containing both constructs were selected on synthetic dropout (SD) medium lacking histidine (–His) and leucine (–Leu) and interaction was assayed on SD –His –Leu plates with 40 mM 3-amino-1,2,4-triazole (3AT).

Protein-binding microarray

For protein production, the EMA1 entry clone was recombined with the pDEST-HisMBP destination vector (Plasmid 11085, Addgene, Cambridge, MA, USA) (Nallamsetty *et al.*, 2005) and the resulting expression clone was transformed into One Shot® *BL21(DE3)* chemically competent *E. coli* (Invitrogen) cells. 25-mL cultures (OD₆₀₀ of 0.5) were treated with 0.4 mM IPTG and further incubated for 4 h at 30°C. Extraction of soluble proteins from induced *E. coli* cultures and identification of the EMA1-binding motifs using a protein-binding microarray was performed as described (Franco-Zorrilla *et al.*, 2014).

Elicitor treatments

M. truncatula (ecotype Jemalong J5) seeds were scarified and sterilized as previously described (Pollier *et al.*, 2011). Sterile seeds were placed on agar plates containing full strength Murashige

and Skoog (MS) medium (pH 5.8) supplemented with vitamins (Duchefa) and placed in the dark for two days at 26°C. Seedlings were then moved to six-well tissue culture plates (Falcon), each well containing three seedlings and four mL of half-strength liquid MS medium (pH 5.8) containing vitamins. Plates were sealed with micropore tape and placed for six days under long day conditions (16h/8h light/dark) at 24°C. For elicitation, the culture medium was replaced with fresh medium containing 200 mM NaCl, 100 µM salicylic acid (Sigma-Aldrich), 100 µM MeJA (Sigma-Aldrich), 100 µM methyl anthranilate (Sigma-Aldrich), 3% (w/v) yeast elicitor, or 1 µM flagellin (flg22, Sigma-Aldrich). Salicylic acid and MeJA stock solutions (1 M) were dissolved in 100% ethanol while all other compounds were dissolved in double distilled water. Yeast elicitor was prepared as reported by (Diwan and Malpathak, 2011). Ethanol was used as mock control. Plants were harvested two and 24 hours after elicitor treatment by freezing intact plants in liquid nitrogen.

ACCESSION NUMBERS

The raw RNA-Seq reads reported in this paper have been deposited in the National Center for Biotechnology Information Short Read Archive with BioProject ID PRJNA498047. Gene sequences can be found in the GenBank database under the following accession numbers: MK570872 (*EMA1*), MK557964 (*MtAAMT1*), and MK557965 (*MtPLATZ1*).

ACKNOWLEDGEMENTS

We thank Jan Mertens for technical assistance, Jan Van Bocxlaer for advice on the volatile profiling, Richard A. Dixon (Samuel Roberts Noble Foundation, Ardmore, USA) for providing the *M. truncatula* cell line and Annick Bleys for help with preparing the article. NDG, TM, YB, and AGh are indebted to the Agency for Innovation by Science and Technology, the VIB International PhD Fellowship Program, the Chinese Scholarship Council (CSC), and the Iranian Ministry for Health and Medical Education, respectively, for predoctoral fellowships. JP is a postdoctoral fellow of the Research Foundation Flanders (FWO).

AUTHOR CONTRIBUTIONS

IW, IY and TT designed the research; SA, TT and IW performed the computational analyses; IW, SS, HE, IY, YF, MA, MB and AD performed the experimental procedures; IW, IY and TT wrote the paper.

JP, NDG, and AG designed the study. JP, NDG, TM, BB, JMFZ, YB, EL, AGh and RVB performed the experiments. JP, NDG, TM, BB, JMFZ, AGh, RVB, DW, SG and AG analyzed the data. AG coordinated the study. All authors contributed to the writing of the manuscript.

CONFLICTS OF INTEREST

No conflicts of interest are to be declared.

REFERENCES

- Battat, M., Eitan, A., Rogachev, I., Hanhineva, K., Fernie, A.R., Tohge, T., Beekwilder, J. and Aharoni, A. (2019) A MYB triad controls primary and phenylpropanoid metabolites for pollen coat patterning. *Plant Physiol.*
- Bernklau, E.J., Hibbard, B.E., Norton, A.P. and Bjostad, L.B. (2016) Methyl anthranilate as a repellent for Western corn rootworm larvae (Coleoptera: Chrysomelidae). *J. Econ. Entomol.* **109**, 1683-1690.
- Boachon, B., Junker, R.R., Miesch, L., Bassard, J.-E., Höfer, R., Caillieudeaux, R., Seidel, D.E., Lesot, A., Heinrich, C., Ginglinger, J.-F., Allouche, L., Vincent, B., Wahyuni, D.S., Paetz, C., Beran, F., Miesch, M., Schneider, B., Leiss, K. and Werck-Reichhart, D. (2015) CYP76C1 (Cytochrome P450)-mediated linalool metabolism and the formation of volatile and soluble linalool oxides in *Arabidopsis* flowers: a strategy for defense against floral antagonists. *Plant Cell* **27**, 2972-2990.

- Broeckling, C.D., Huhman, D.V., Farag, M.A., Smith, J.T., May, G.D., Mendes, P., Dixon, R.A. and Sumner, L.W.** (2005) Metabolic profiling of *Medicago truncatula* cell cultures reveals the effects of biotic and abiotic elicitors on metabolism. *J. Exp. Bot.* **56**, 323-336.
- Chambers, A.H., Evans, S.A. and Folta, K.M.** (2013) Methyl anthranilate and γ -decalactone inhibit strawberry pathogen growth and achene germination. *J. Agric. Food Chem.* **61**, 12625-12633.
- Cheng, H., Song, S., Xiao, L., Soo, H.M., Cheng, Z., Xie, D. and Peng, J.** (2009) Gibberellin acts through jasmonate to control the expression of *MYB21*, *MYB24*, and *MYB57* to promote stamen filament growth in *Arabidopsis*. *PLoS Genet.* **5**, e1000440.
- Chezem, W.R. and Clay, N.K.** (2016) Regulation of plant secondary metabolism and associated specialized cell development by MYBs and bHLHs. *Phytochemistry* **131**, 26-43.
- Chini, A., Fonseca, S., Fernández, G., Adie, B., Chico, J.M., Lorenzo, O., García-Casado, G., López-Vidriero, I., Lozano, F.M., Ponce, M.R., Micol, J.L. and Solano, R.** (2007) The JAZ family of repressors is the missing link in jasmonate signalling. *Nature* **448**, 666-671.
- Chini, A., Gimenez-Ibanez, S., Goossens, A. and Solano, R.** (2016) Redundancy and specificity in jasmonate signalling. *Curr. Opin. Plant Biol.* **33**, 147-156.
- Colinas, M. and Goossens, A.** (2018) Combinatorial transcriptional control of plant specialized metabolism. *Trends Plant Sci.* **23**, 324-336.
- Colling, J., Tohge, T., De Clercq, R., Brunoud, G., Vernoux, T., Fernie, A.R., Makunga, N.P., Goossens, A. and Pauwels, L.** (2015) Overexpression of the *Arabidopsis thaliana* signalling peptide TAXIMIN1 affects lateral organ development. *J. Exp. Bot.* **66**, 5337-5349.
- Colquhoun, T.A., Kim, J.Y., Wedde, A.E., Levin, L.A., Schmitt, K.C., Schuurink, R.C. and Clark, D.G.** (2011) *PhMYB4* fine-tunes the floral volatile signature of *Petunia* \times *hybrida* through *PhC4H*. *J. Exp. Bot.* **62**, 1133-1143.
- De Geyter, N., Gholami, A., Goormachtig, S. and Goossens, A.** (2012) Transcriptional machineries in jasmonate-elicited plant secondary metabolism. *Trends Plant Sci.* **17**, 349-359.
- De Sutter, V., Vanderhaeghen, R., Tilleman, S., Lammertyn, F., Vanhoutte, I., Karimi, M., Inzé, D., Goossens, A. and Hilson, P.** (2005) Exploration of jasmonate signalling via automated and standardized transient expression assays in tobacco cells. *The Plant Journal* **44**, 1065-1076.
- Deplancke, B., Dupuy, D., Vidal, M. and Walhout, A.J.M.** (2004) A gateway-compatible yeast one-hybrid system. *Genome Res.* **14**, 2093-2101.
- Diwan, R. and Malpathak, N.** (2011) Bioprocess optimization of furanocoumarin elicitation by medium renewal and re-elicitation: a perfusion-based approach. *Appl. Biochem. Biotechnol.* **163**, 756-764.
- Dubos, C., Stracke, R., Grotewold, E., Weisshaar, B., Martin, C. and Lepiniec, L.** (2010) MYB transcription factors in *Arabidopsis*. *Trends Plant Sci.* **15**, 573-581.
- Dudareva, N., Klempien, A., Muhlemann, J.K. and Kaplan, I.** (2013) Biosynthesis, function and metabolic engineering of plant volatile organic compounds. *New Phytol.* **198**, 16-32.
- Esther, A., Tilcher, R. and Jacob, J.** (2013) Assessing the effects of three potential chemical repellents to prevent bird damage to corn seeds and seedlings. *Pest Manag. Sci.* **69**, 425-430.
- Franco-Zorrilla, J.M., López-Vidriero, I., Carrasco, J.L., Godoy, M., Vera, P. and Solano, R.** (2014) DNA-binding specificities of plant transcription factors and their potential to define target genes. *Proc. Natl. Acad. Sci. USA* **111**, 2367-2372.
- Gholami, A., De Geyter, N., Pollier, J., Goormachtig, S. and Goossens, A.** (2014) Natural product biosynthesis in *Medicago* species. *Nat. Prod. Rep.* **31**, 356-380.
- Godoy, M., Franco-Zorrilla, J.M., Pérez-Pérez, J., Oliveros, J.C., Lorenzo, O. and Solano, R.** (2011) Improved protein-binding microarrays for the identification of DNA-binding specificities of transcription factors. *Plant J.* **66**, 700-711.
- Gols, R.** (2014) Direct and indirect chemical defences against insects in a multitrophic framework. *Plant Cell Environ.* **37**, 1741-1752.
- Goossens, J., Fernández-Calvo, P., Schweizer, F. and Goossens, A.** (2016) Jasmonates: signal transduction components and their roles in environmental stress responses. *Plant Mol. Biol.* **91**, 673-689.
- Goossens, J., Mertens, J. and Goossens, A.** (2017) Role and functioning of bHLH transcription factors in jasmonate signalling. *J. Exp. Bot.* **68**, 1333-1347.
- He, J., Benedito, V.A., Wang, M., Murray, J.D., Zhao, P.X., Tang, Y. and Udvardi, M.K.** (2009) The *Medicago truncatula* gene expression atlas web server. *BMC Bioinformatics* **10**, 441.
- Hong, G.-J., Xue, X.-Y., Mao, Y.-B., Wang, L.-J. and Chen, X.-Y.** (2012) *Arabidopsis* MYC2 interacts with DELLA proteins in regulating sesquiterpene synthase gene expression. *Plant Cell* **24**, 2635-2648.
- Huang, M., Sanchez-Moreiras, A.M., Abel, C., Sohrabi, R., Lee, S., Gershenzon, J. and Tholl, D.** (2012) The major volatile organic compound emitted from *Arabidopsis thaliana* flowers, the sesquiterpene (*E*)- β -caryophyllene, is a defense against a bacterial pathogen. *New Phytol.* **193**, 997-1008.

- Kant, M.R., Ament, K., Sabelis, M.W., Haring, M.A. and Schuurink, R.C.** (2004) Differential timing of spider mite-induced direct and indirect defenses in tomato plants. *Plant Physiol.* **135**, 483-495.
- Karimi, M., Inzé, D. and Depicker, A.** (2002) GATEWAY™ vectors for *Agrobacterium*-mediated plant transformation. *Trends Plant Sci.* **7**, 193-195.
- Kim, J.H., Kim, J., Jun, S.E., Park, S., Timilsina, R., Kwon, D.S., Kim, Y., Park, S.-J., Hwang, J.Y., Nam, H.G., Kim, G.-T. and Woo, H.R.** (2018) ORESARA15, a PLATZ transcription factor, mediates leaf growth and senescence in *Arabidopsis*. *New Phytol.* **220**, 609-623.
- Köllner, T.G., Lenk, C., Zhao, N., Seidl-Adams, I., Gershenzon, J., Chen, F. and Degenhardt, J.** (2010) Herbivore-induced SABATH methyltransferases of maize that methylate anthranilic acid using S-adenosyl-L-methionine. *Plant Physiol.* **153**, 1795-1807.
- Kozbial, P.Z. and Mushegian, A.R.** (2005) Natural history of S-adenosylmethionine-binding proteins. *BMC Struct. Biol.* **5**, 19.
- Kranz, H.D., Denekamp, M., Greco, R., Jin, H., Leyva, A., Meissner, R.C., Petroni, K., Urzainqui, A., Bevan, M., Martin, C., Smeekens, S., Tonelli, C., Paz-Ares, J. and Weisshaar, B.** (1998) Towards functional characterisation of the members of the *R2R3-MYB* gene family from *Arabidopsis thaliana*. *Plant J.* **16**, 263-276.
- Lescot, M., Déhais, P., Thijs, G., Marchal, K., Moreau, Y., Van de Peer, Y., Rouzé, P. and Rombauts, S.** (2002) PlantCARE, a database of plant cis-acting regulatory elements and a portal to tools for *in silico* analysis of promoter sequences. *Nucleic Acids Res.* **30**, 325-327.
- Li, Q., Wang, J., Ye, J., Zheng, X., Xiang, X., Li, C., Fu, M., Wang, Q., Zhang, Z. and Wu, Y.** (2017a) The maize imprinted gene *floury3* encodes a PLATZ protein required for tRNA and 5S rRNA transcription through interaction with RNA polymerase III. *Plant Cell* **29**, 2661-2675.
- Li, X., Xu, Y., Shen, S., Yin, X., Klee, H., Zhang, B. and Chen, K.** (2017b) Transcription factor CitERF71 activates the terpene synthase gene *CitTPS16* involved in the synthesis of *E*-geraniol in sweet orange fruit. *J. Exp. Bot.* **68**, 4929-4938.
- Lin, J., Mazarei, M., Zhao, N., Zhu, J.J., Zhuang, X., Liu, W., Pantalone, V.R., Arelli, P.R., Stewart, C.N. and Chen, F.** (2013) Overexpression of a soybean salicylic acid methyltransferase gene confers resistance to soybean cyst nematode. *Plant Biotechnol. J.* **11**, 1135-1145.
- Mandaokar, A. and Browse, J.** (2009) MYB108 acts together with MYB24 to regulate jasmonate-mediated stamen maturation in *Arabidopsis*. *Plant Physiol.* **149**, 851-862.
- Medina-Puche, L., Molina-Hidalgo, F.J., Boersma, M., Schuurink, R.C., López-Vidriero, I., Solano, R., Franco-Zorrilla, J.-M., Caballero, J.L., Blanco-Portales, R. and Muñoz-Blanco, J.** (2015) A R2R3-MYB transcription factor regulates eugenol production in ripe strawberry fruit receptacles. *Plant Physiol.* **168**, 598-614.
- Mertens, J., Pollier, J., Vanden Bossche, R., Lopez-Vidriero, I., Franco-Zorrilla, J.M. and Goossens, A.** (2016a) The bHLH transcription factors TSAR1 and TSAR2 regulate triterpene saponin biosynthesis in *Medicago truncatula*. *Plant Physiol.* **170**, 194-210.
- Mertens, J., Van Moerkercke, A., Vanden Bossche, R., Pollier, J. and Goossens, A.** (2016b) Clade IVa basic helix-loop-helix transcription factors form part of a conserved jasmonate signaling circuit for the regulation of bioactive plant terpenoid biosynthesis. *Plant Cell Physiol.* **57**, 2564-2575.
- Mithöfer, A. and Boland, W.** (2012) Plant defense against herbivores: chemical aspects. *Annu. Rev. Plant Biol.* **63**, 431-450.
- Muhlemann, J.K., Klempien, A. and Dudareva, N.** (2014) Floral volatiles: from biosynthesis to function. *Plant Cell Environ.* **37**, 1936-1949.
- Nagano, Y., Furuhashi, H., Inaba, T. and Sasaki, Y.** (2001) A novel class of plant-specific zinc-dependent DNA-binding protein that binds to A/T-rich DNA sequences. *Nucleic Acids Res.* **29**, 4097-4105.
- Nallamsetty, S., Austin, B.P., Penrose, K.J. and Waugh, D.S.** (2005) Gateway vectors for the production of combinatorially-tagged His₆-MBP fusion proteins in the cytoplasm and periplasm of *Escherichia coli*. *Protein Sci.* **14**, 2964-2971.
- Naoumkina, M., Farag, M.A., Sumner, L.W., Tang, Y., Liu, C.-J. and Dixon, R.A.** (2007) Different mechanisms for phytoalexin induction by pathogen and wound signals in *Medicago truncatula*. *Proc. Natl. Acad. Sci. USA* **104**, 17909-17915.
- Negre, F., Kolosova, N., Knoll, J., Kish, C.M. and Dudareva, N.** (2002) Novel S-adenosyl-L-methionine:salicylic acid carboxyl methyltransferase, an enzyme responsible for biosynthesis of methyl salicylate and methyl benzoate, is not involved in floral scent production in snapdragon flowers. *Arch. Biochem. Biophys.* **406**, 261-270.
- Niyogi, K.K. and Fink, G.R.** (1992) Two anthranilate synthase genes in *Arabidopsis*: defense-related regulation of the tryptophan pathway. *The Plant Cell* **4**, 721-733.
- Niyogi, K.K., Last, R.L., Fink, G.R. and Keith, B.** (1993) Suppressors of *trp1* fluorescence identify a new *Arabidopsis* gene, TRP4, encoding the anthranilate synthase beta subunit. *The Plant Cell* **5**, 1011-1027.

- Ohta, M., Ohme-Takagi, M. and Shinshi, H. (2000) Three ethylene-responsive transcription factors in tobacco with distinct transactivation functions. *Plant J.* **22**, 29-38.
- Onrubia, M., Pollier, J., Vanden Bossche, R., Goethals, M., Gevaert, K., Moyano, E., Vidal-Limon, H., Cusidó, R.M., Palazón, J. and Goossens, A. (2014) Taximin, a conserved plant-specific peptide is involved in the modulation of plant-specialized metabolism. *Plant Biotechnol. J.* **12**, 971-983.
- Pauwels, L., Inzé, D. and Goossens, A. (2009) Jasmonate-inducible gene: What does it mean? *Trends Plant Sci.* **14**, 87-91.
- Pauwels, L. and Goossens, A. (2011) The JAZ proteins: a crucial interface in the jasmonate signaling cascade. *Plant Cell* **23**, 3089-3100.
- Pichersky, E. and Lewinsohn, E. (2011) Convergent evolution in plant specialized metabolism. *Annu. Rev. Plant Biol.* **62**, 549-566.
- Pierik, R., Ballaré, C.L. and Dicke, M. (2014) Ecology of plant volatiles: taking a plant community perspective. *Plant Cell Environ.* **37**, 1845-1853.
- Pillet, J., Chambers, A.H., Barbey, C., Bao, Z., Plotto, A., Bai, J., Schwieterman, M., Johnson, T., Harrison, B., Whitaker, V.M., Colquhoun, T.A. and Folta, K.M. (2017) Identification of a methyltransferase catalyzing the final step of methyl anthranilate synthesis in cultivated strawberry. *BMC Plant Biol.* **17**, 147.
- Pollier, J., Morreel, K., Geelen, D. and Goossens, A. (2011) Metabolite profiling of triterpene saponins in *Medicago truncatula* hairy roots by liquid chromatography Fourier transform ion cyclotron resonance mass spectrometry. *J. Nat. Prod.* **74**, 1462-1476.
- Pollier, J. and Goossens, A. (2013) Metabolite profiling of plant tissues by liquid chromatography Fourier transform ion cyclotron resonance mass spectrometry. *Methods Mol. Biol.* **1011**, 277-286.
- Pollier, J., Moses, T., González-Guzmán, M., De Geyter, N., Lippens, S., Vanden Bossche, R., Marhavý, P., Kremer, A., Morreel, K., Guérin, C.J., Tava, A., Oleszek, W., Thevelein, J.M., Campos, N., Goormachtig, S. and Goossens, A. (2013a) The protein quality control system manages plant defence compound synthesis. *Nature* **504**, 148-152.
- Pollier, J., Rombauts, S. and Goossens, A. (2013b) Analysis of RNA-Seq data with TopHat and Cufflinks for genome-wide expression analysis of jasmonate-treated plants and plant cultures. *Methods Mol. Biol.* **1101**, 305-315.
- Ponzio, C., Gols, R., Weldegergis, B.T. and Dicke, M. (2014) Caterpillar-induced plant volatiles remain a reliable signal for foraging wasps during dual attack with a plant pathogen or non-host insect herbivore. *Plant Cell Environ.* **37**, 1924-1935.
- Pott, M.B., Hippauf, F., Saschenbrecker, S., Chen, F., Ross, J., Kiefer, I., Slusarenko, A., Noel, J.P., Pichersky, E., Effmert, U. and Piechulla, B. (2004) Biochemical and structural characterization of benzenoid carboxyl methyltransferases involved in floral scent production in *Stephanotis floribunda* and *Nicotiana suaveolens*. *Plant Physiol.* **135**, 1946-1955.
- Reddy, V.A., Wang, Q., Dhar, N., Kumar, N., Venkatesh, P.N., Rajan, C., Panicker, D., Sridhar, V., Mao, H.-Z. and Sarojam, R. (2017) Spearmint R2R3-MYB transcription factor MsMYB negatively regulates monoterpene production and suppresses the expression of geranyl diphosphate synthase large subunit (*MsGPPS.LSU*). *Plant Biotechnol. J.* **15**, 1105-1119.
- Reeves, P.H., Ellis, C.M., Ploense, S.E., Wu, M.-F., Yadav, V., Tholl, D., Chételat, A., Haupt, I., Kennerley, B.J., Hodgens, C., Farmer, E.E., Nagpal, P. and Reed, J.W. (2012) A regulatory network for coordinated flower maturation. *PLoS Genet.* **8**, e1002506.
- Robacker, D.C., Massa, M.J., Sacchetti, P. and Bartelt, R.J. (2011) A novel attractant for *Anastrepha ludens* (Diptera: Tephritidae) from a Concord grape product. *J. Econ. Entomol.* **104**, 1195-1203.
- Ross, J.R., Nam, K.H., D'Auria, J.C. and Pichersky, E. (1999) S-Adenosyl-L-methionine:salicylic acid carboxyl methyltransferase, an enzyme involved in floral scent production and plant defense, represents a new class of plant methyltransferases. *Arch. Biochem. Biophys.* **367**, 9-16.
- Saikumar, P., Murali, R. and Reddy, E.P. (1990) Role of tryptophan repeats and flanking amino acids in Myb-DNA interactions. *Proc. Natl. Acad. Sci. USA* **87**, 8452-8456.
- Smith, C.A., Want, E.J., O'Maille, G., Abagyan, R. and Siuzdak, G. (2006) XCMS: processing mass spectrometry data for metabolite profiling using Nonlinear peak alignment, matching, and identification. *Anal. Chem.* **78**, 779-787.
- Song, S., Qi, T., Huang, H., Ren, Q., Wu, D., Chang, C., Peng, W., Liu, Y., Peng, J. and Xie, D. (2011) The Jasmonate-ZIM domain proteins interact with the R2R3-MYB transcription factors MYB21 and MYB24 to affect jasmonate-regulated stamen development in *Arabidopsis*. *Plant Cell* **23**, 1000-1013.
- Spitzer-Rimon, B., Marhevka, E., Barkai, O., Marton, I., Edelbaum, O., Masci, T., Prathapani, N.-K., Shklarman, E., Ovadis, M. and Vainstein, A. (2010) *EOBII*, a gene encoding a flower-specific regulator of phenylpropanoid volatiles' biosynthesis in petunia. *Plant Cell* **22**, 1961-1976.

- Spitzer-Rimon, B., Farhi, M., Albo, B., Cna'ani, A., Ben Zvi, M.M., Masci, T., Edelbaum, O., Yu, Y., Shklarman, E., Ovadis, M. and Vainstein, A.** (2012) The R2R3-MYB-like regulatory factor EOBI, acting downstream of EOBI, regulates scent production by activating *ODO1* and structural scent-related genes in petunia. *Plant Cell* **24**, 5089-5105.
- Stracke, R., Werber, M. and Weisshaar, B.** (2001) The *R2R3-MYB* gene family in *Arabidopsis thaliana*. *Curr. Opin. Plant Biol.* **4**, 447-456.
- Suzuki, H., Achnine, L., Xu, R., Matsuda, S.P.T. and Dixon, R.A.** (2002) A genomics approach to the early stages of triterpene saponin biosynthesis in *Medicago truncatula*. *Plant J.* **32**, 1033-1048.
- Suzuki, H., Reddy, M.S.S., Naoumkina, M., Aziz, N., May, G.D., Huhman, D.V., Sumner, L.W., Blount, J.W., Mendes, P. and Dixon, R.A.** (2005) Methyl jasmonate and yeast elicitor induce differential transcriptional and metabolic re-programming in cell suspension cultures of the model legume *Medicago truncatula*. *Planta* **220**, 696-707.
- Tamura, K., Peterson, D., Peterson, N., Stecher, G., Nei, M. and Kumar, S.** (2011) MEGA5: molecular evolutionary genetics analysis using maximum likelihood, evolutionary distance, and maximum parsimony methods. *Mol. Biol. Evol.* **28**, 2731-2739.
- Tang, H., Krishnakumar, V., Bidwell, S., Rosen, B., Chan, A., Zhou, S., Gentzittel, L., Childs, K.L., Yandell, M., Gundlach, H., Mayer, K.F.X., Schwartz, D.C. and Town, C.D.** (2014) An improved genome release (version Mt4.0) for the model legume *Medicago truncatula*. *BMC Genomics* **15**, 312.
- Tieman, D., Zeigler, M., Schmelz, E., Taylor, M.G., Rushing, S., Jones, J.B. and Klee, H.J.** (2010) Functional analysis of a tomato salicylic acid methyl transferase and its role in synthesis of the flavor volatile methyl salicylate. *Plant J.* **62**, 113-123.
- Trapnell, C., Pachter, L. and Salzberg, S.L.** (2009) TopHat: discovering splice junctions with RNA-Seq. *Bioinformatics* **25**, 1105-1111.
- Trapnell, C., Williams, B.A., Pertea, G., Mortazavi, A., Kwan, G., van Baren, M.J., Salzberg, S.L., Wold, B.J. and Pachter, L.** (2010) Transcript assembly and quantification by RNA-Seq reveals unannotated transcripts and isoform switching during cell differentiation. *Nat. Biotechnol.* **28**, 511-515.
- Van Moerkercke, A., Haring, M.A. and Schuurink, R.C.** (2011) The transcription factor EMISSION OF BENZENOIDS II activates the MYB *ODORANT1* promoter at a MYB binding site specific for fragrant petunias. *Plant J.* **67**, 917-928.
- Vanden Bossche, R., Demedts, B., Vanderhaeghen, R. and Goossens, A.** (2013) Transient expression assays in tobacco protoplasts. *Methods Mol. Biol.* **1101**, 227-239.
- Verdonk, J.C., Haring, M.A., van Tunen, A.J. and Schuurink, R.C.** (2005) *ODORANT1* regulates fragrance biosynthesis in petunia flowers. *Plant Cell* **17**, 1612-1624.
- Wang, J. and De Luca, V.** (2005) The biosynthesis and regulation of biosynthesis of Concord grape fruit esters, including 'foxy' methylanthranilate. *Plant J.* **44**, 606-619.
- Wang, J., Ji, C., Li, Q., Zhou, Y. and Wu, Y.** (2018) Genome-wide analysis of the plant-specific PLATZ proteins in maize and identification of their general role in interaction with RNA polymerase III complex. *BMC Plant Biol.* **18**, 221.
- Wasternack, C. and Hause, B.** (2013) Jasmonates: biosynthesis, perception, signal transduction and action in plant stress response, growth and development. An update to the 2007 review in *Annals of Botany*. *Ann. Bot.* **111**, 1021-1058.
- Wasternack, C. and Song, S.** (2017) Jasmonates: biosynthesis, metabolism, and signaling by proteins activating and repressing transcription. *J. Exp. Bot.* **68**, 1303-1321.
- Wasternack, C. and Strnad, M.** (2018) Jasmonates are signals in the biosynthesis of secondary metabolites — Pathways, transcription factors and applied aspects — A brief review. *New Biotechnol.* in press (10.1016/j.nbt.2017.09.007).
- Zhang, S., Yang, R., Huo, Y., Liu, S., Yang, G., Huang, J., Zheng, C. and Wu, C.** (2018) Expression of cotton PLATZ1 in transgenic *Arabidopsis* reduces sensitivity to osmotic and salt stress for germination and seedling establishment associated with modification of the abscisic acid, gibberellin, and ethylene signalling pathways. *BMC Plant Biol.* **18**, 218.
- Zhao, N., Yao, J., Chaiprasongsuk, M., Li, G., Guan, J., Tschapinski, T.J., Guo, H. and Chen, F.** (2013) Molecular and biochemical characterization of the jasmonic acid methyltransferase gene from black cottonwood (*Populus trichocarpa*). *Phytochemistry* **94**, 74-81.
- Zhou, M. and Memelink, J.** (2016) Jasmonate-responsive transcription factors regulating plant secondary metabolism. *Biotechnol. Adv.* **34**, 441-449.

TABLES

Table 1. Genes with higher expression in the EMA1^{OE} lines as compared to the control lines.

Gene	FPKM CTR	FPKM EMA1	p-value	Annotation
<i>Medtr4g094680</i>	0	10.1532	1.95E-06	PLATZ transcription factor
<i>Medtr1g086530</i>	1.25087	171.541	9.55E-09	EMA1
<i>Medtr4g006650</i>	0.911663	21.6298	1.33E-04	Aquaporin NIP6-1
<i>Medtr4g018820</i>	21.0721	275.4	2.26E-07	Jasmonate <i>O</i> -methyltransferase
<i>Medtr6g059650</i>	21.0048	234.081	7.16E-07	Kunitz-type trypsin inhibitor
<i>Medtr8g018650</i>	9.87718	72.0369	5.21E-06	Lipoxygenase
<i>Medtr2g090245</i>	27.9787	124.374	8.02E-05	Epoxide hydrolase

FIGURES

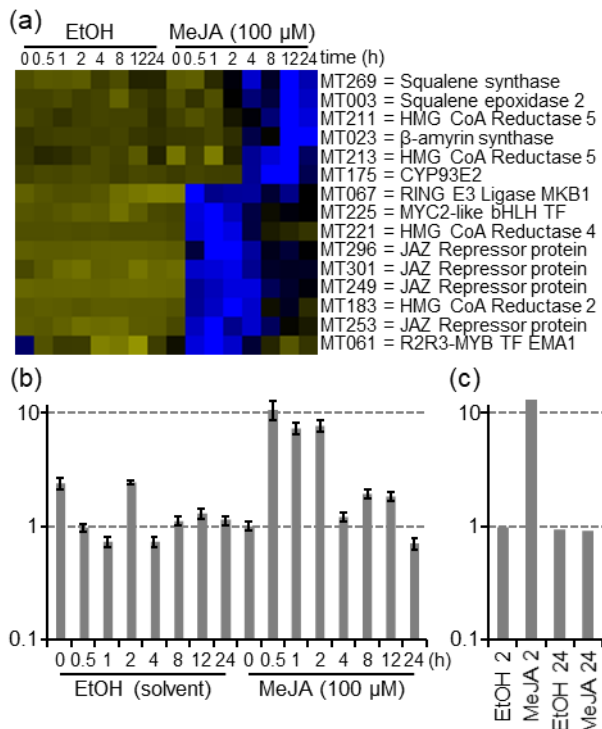


Figure 1. Increased transcript levels of *EMA1* in *M. truncatula* suspension cells treated with 100 μ M of MeJA (dissolved in ethanol) or an equivalent amount of ethanol as control. (a) Subcluster of the *M. truncatula* transcriptome (Pollier *et al.*, 2013a) comprising genes involved in triterpene biosynthesis or JA signaling. Treatments and time points (in h) are indicated on top. Increased and decreased expression levels relative to the average expression level are reflected by blue and yellow boxes, respectively. (b) qPCR analysis of *EMA1* in MeJA-treated *M. truncatula* suspension cells. The graph shows the relative gene expression of *EMA1* in log scale, normalized to the *EMA1* transcript levels of the MeJA 0 sample (error bars indicate SEM, $n = 3$ technical replicates). Treatments and time points (in h) are indicated in the x-axis. (c) Expression of *EMA1* in MeJA-treated *M. truncatula* cells according to the *M. truncatula* gene expression atlas (He *et al.*, 2009). The graph shows the relative gene expression of *EMA1* in log scale, normalized to the transcript levels of the sample taken after a 2-h treatment with EtOH. Treatments and time points (in h) are indicated in the x-axis.

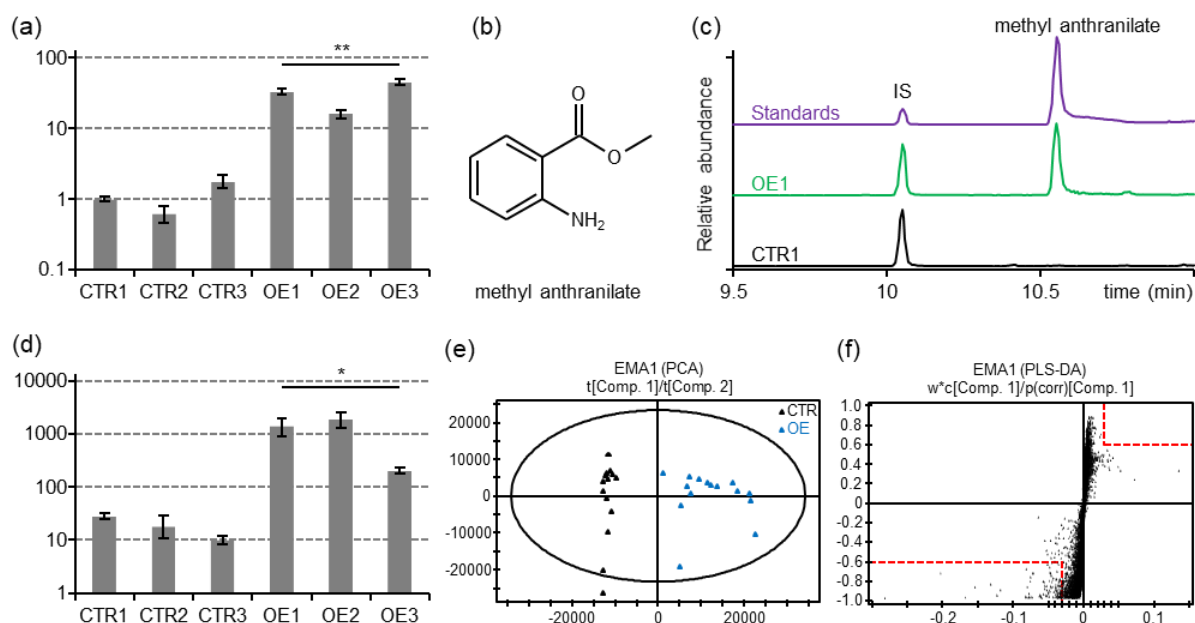


Figure 2. Overexpression of *EMA1* in *M. truncatula* hairy roots leads to the emission of methyl anthranilate. (a) qPCR analysis of *EMA1* gene expression in three independent *EMA1*^{OE} (OE) and control (CTR) hairy root lines. The graph shows the relative gene expression of *EMA1* in log scale, normalized to the *EMA1* transcript levels in control line 1 (error bars indicate SEM, n = 3 technical replicates). Statistical significance was determined by a Student's *t*-test (***p*<0.01). (b) Chemical structure of methyl anthranilate. (c) GC-MS chromatograms of the volatiles emitted by three independent control (CTR, black) and *EMA1*^{OE} (OE, green) hairy root lines. The major differential compound corresponds to methyl anthranilate. A methyl anthranilate standard (purple) was analyzed along with the hairy roots samples. IS; internal standard (nonyl acetate) (d) Quantification of methyl anthranilate emission in three independent control (CTR) and *EMA1*^{OE} (OE) lines. The graph shows the emission of methyl anthranilate in ng per h per g of roots in log scale, normalized against the internal standard (error bars indicate SEM, n = 3 technical replicates). Statistical significance was determined by a Student's *t*-test (**p*<0.05). (e) Principal component analysis projecting the first (t[Comp. 1]) and second (t[Comp. 2]) principal components of the metabolite profiling analysis of three independent *EMA1*^{OE} (blue) and CTR (black) roots. (f) S-plot for correlation (p[corr][1]) and covariance (w*c[1]) derived from partial least squares discriminant analysis. Metabolites in the bottom left and top right quadrants (marked by dashed red lines) are significantly higher or lower, respectively, in abundance in the *EMA1*^{OE} lines. Metabolite identifications are presented in Data S1.

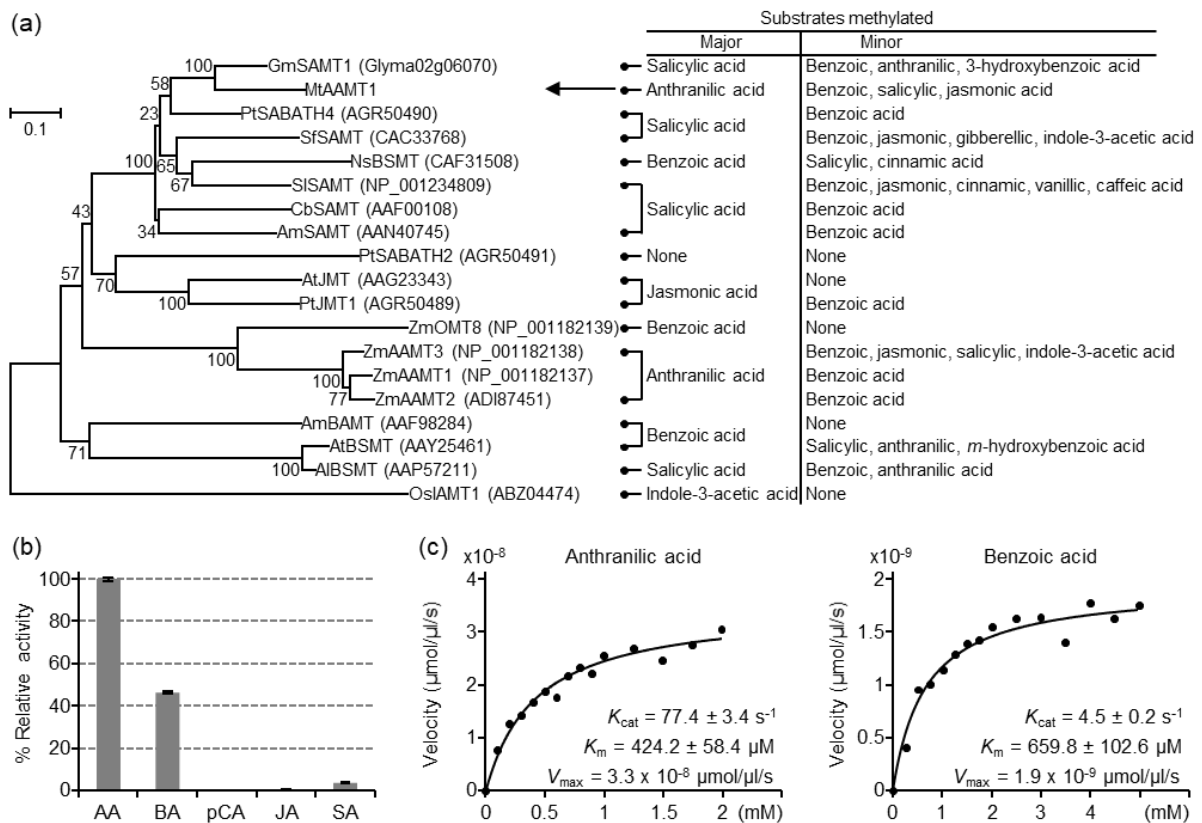


Figure 3. Functional characterization of *M. truncatula* Medtr4g018820 (MtAAMT1). (a) Phylogenetic analysis of MtAAMT1 and other SABATH methyltransferases involved in methylation of small acids. The percentage of replicate trees that clustered together in the bootstrap test is indicated at the branches and the scale bar corresponds to the number of amino acid substitutions per site. The major and minor substrates methylated by the methyltransferases are indicated on the right. The amino acid sequences were retrieved from GenBank. MtAAMT1 characterized in this study is indicated with an arrow. Al, *Arabidopsis lyrata*; Am, *Antirrhinum majus*; At, *Arabidopsis thaliana*; Cb, *Clarkia breweri*; Gm, *Glycine max*; Mt, *Medicago truncatula*; Ns, *Nicotiana suaveolens*; Os, *Oryza sativa*; Pt, *Populus trichocarpa*; Sf, *Stephanotis floribunda*; Sl, *Solanum lycopersicum*; Zm, *Zea mays*. (b) Relative enzyme activity of MtAAMT1 with 1 mM of five small acid substrates. Error bars indicate SEM ($n = 3$ technical replicates). AA, anthranilic acid; BA, benzoic acid; pCA, p-coumaric acid; JA, jasmonic acid; SA, salicylic acid. (c) Steady-state kinetic analysis of MtAAMT1 assayed with anthranilic acid (left) and benzoic acid (right). Initial velocities are shown as dots. The curve represents the nonlinear least-squares fit of the initial velocities versus substrate concentration to the hyperbolic Michaelis-Menten equation. V_{max} , K_m and K_{cat} values are given in the plots.

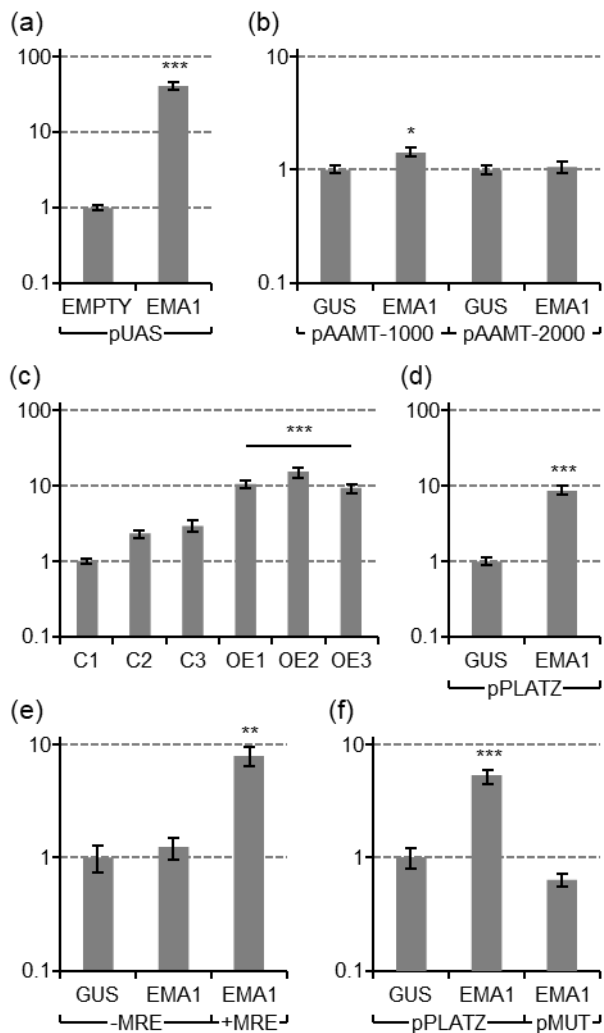


Figure 4. The transcriptional activator EMA1 activates the *MtPLATZ1* promoter and not the *MtAAMT1* promoter. (a) Transient expression assay in tobacco protoplasts showing the transcriptional activation of the *UAS* promoter (pUAS) driving *firefly luciferase* (*fLUC*) expression by co-transfection of the protoplasts with an effector plasmid expressing *EMA1* fused in-frame to the *GAL4* DNA-binding domain. Values in the y-axis are normalized fold changes in log scale relative to protoplasts co-transfected with the pUAS and an empty effector plasmid. (b) Transient expression assay in tobacco protoplasts co-transfected with an effector plasmid expressing *EMA1* and either the 1000-bp or the 2000-bp *MtAAMT1* promoters driving *fLUC* expression. Values in the y-axis are normalized fold changes in log scale relative to protoplasts co-transfected with the reporter construct and a pCaMV35S:*GUS* (*GUS*) control plasmid. (c) qPCR analysis showing transcriptional activation of *MtPLATZ1* in three independent *EMA1*^{OE} (OE) hairy root lines compared to three independent control (C) hairy root lines. Error bars indicate SE; n = 3 technical replicates. (d) Transient expression assay in tobacco protoplasts showing transcriptional activation of the 1000-bp *MtPLATZ1* promoter (pPLATZ) driving *fLUC* expression by co-transfection of the protoplasts with an effector plasmid expressing *EMA1*. Values in the y-axis are normalized fold changes in log scale relative to protoplasts co-transfected with the reporter construct and a pCaMV35S:*GUS* (*GUS*) control plasmid. (e) Transient expression assay in tobacco protoplasts showing transcriptional activation of the 198-bp *MtPLATZ1* promoter (+MRE), but not of the 149-bp *MtPLATZ1* promoter (-MRE), driving *fLUC* expression by co-transfection of the protoplasts with an effector plasmid expressing *EMA1*. Values in the y-axis are normalized fold changes in log scale relative to protoplasts co-transfected with the -MRE reporter construct and a

pCaMV35S:GUS (GUS) control plasmid. (f) Transient expression assay in tobacco protoplasts showing transcriptional activation of the 1000-bp *MtPLATZ1* promoter (pPLATZ), but not of the 1000-bp *MtPLATZ* promoter in which the MRE domain was mutated (pMUT), driving *fLUC* expression by co-transfection of the protoplasts with an effector plasmid expressing *EMAI*. Values in the y-axis are normalized fold changes in log scale relative to protoplasts co-transfected with the reporter construct and a pCaMV35S:GUS (GUS) control plasmid. For the normalization procedure of the protoplast assays, see the methods section. For all protoplast assays, error bars indicate SEM; n = 8 biological replicates. Statistical significances were determined by a Student's *t*-test (*p<0.05, **p<0.01, ***p<0.001).

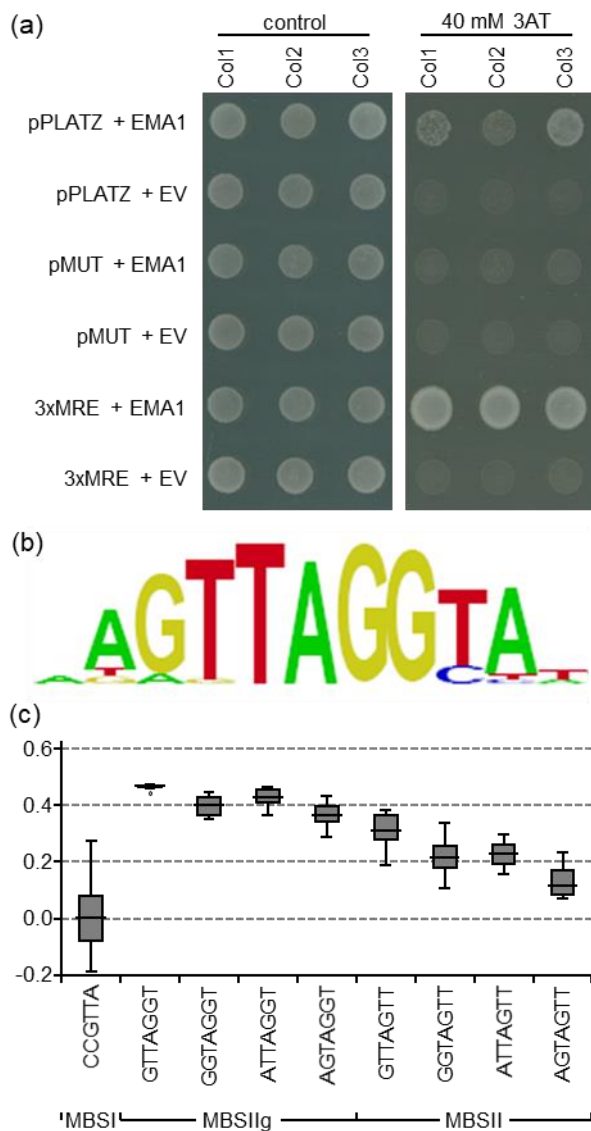


Figure 5. EMA1 binds the *MtPLATZ1* promoter through a repeated ACCTAAC motif. (a) Yeast one-hybrid assay showing binding of the EMA1 transcription factor on the MRE-element of the *MtPLATZ1* promoter. Yeast growth was observed with the wild-type *MtPLATZ1* promoter (pPLATZ) fragment, but not with the *MtPLATZ1* promoter fragment in which the MRE-element was mutated (pMUT). Strong yeast growth was observed with a synthetic DNA fragment containing a triple repeat of the MRE-element (3xMRE). EV = empty vector control. (b) Position weight matrix representation of the top-scoring motif in the protein-binding microarray of EMA1. (c) Box-and-Whisker plot showing the E-score distributions of 8-mers containing DNA elements recognized by R2R3-MYBs (MBSI, MBSIIg, MBSII).

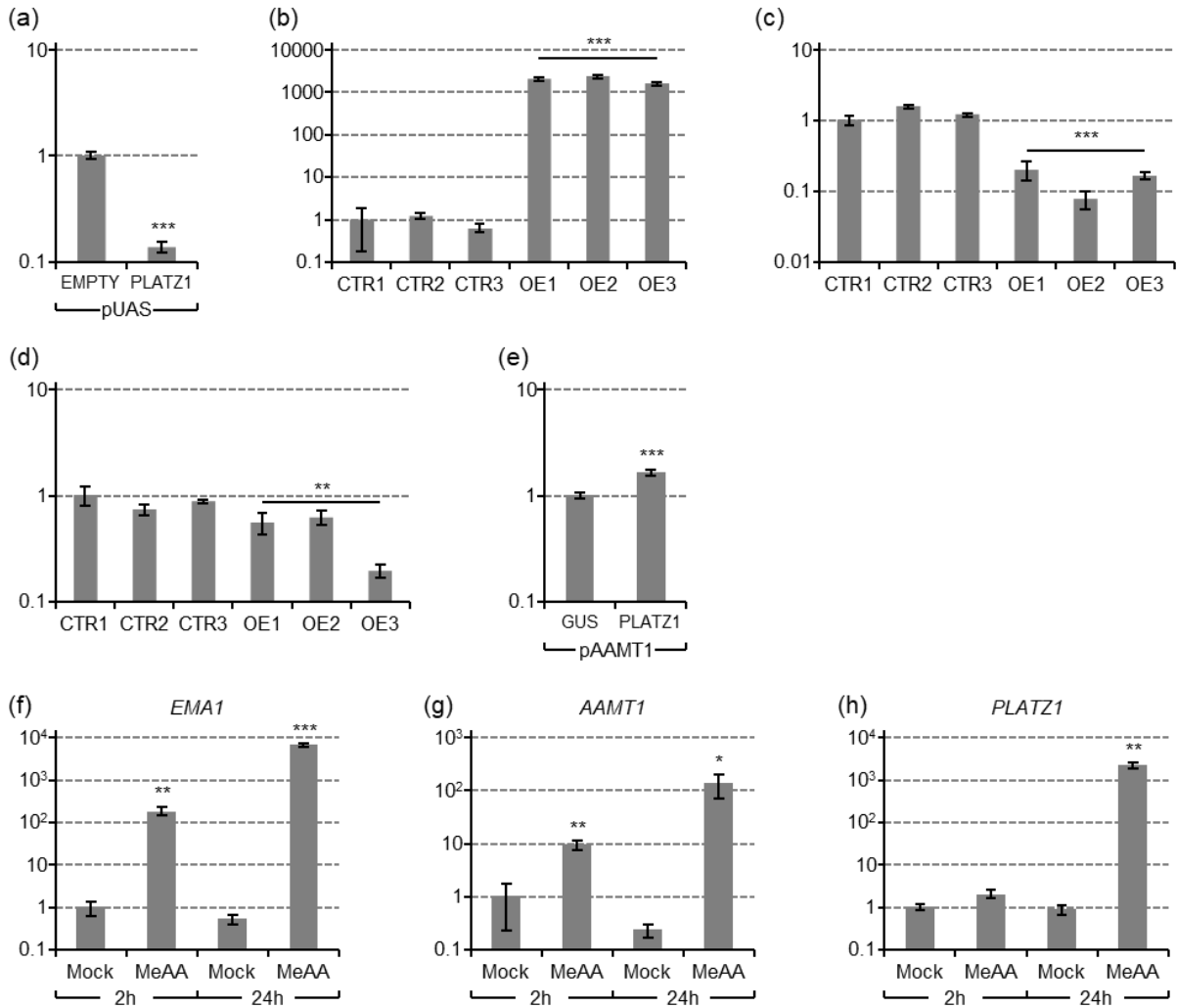


Figure 6. Overexpression of the transcriptional repressor *MtPLATZ1* in *M. truncatula* hairy roots leads to reduced expression of *EMA1*. (a) Transient expression assay in tobacco protoplasts showing the transcriptional repression of the *UAS* promoter (pUAS) driving *firefly luciferase* (*fLUC*) expression by co-transfection of the protoplasts with an effector plasmid expressing *MtPLATZ1* fused in-frame to the GAL4 DNA-binding domain. Values in the y-axis are normalized fold changes in log scale relative to protoplasts co-transfected with the pUAS and an empty effector plasmid. Error bars indicate SEM; n = 8 biological replicates. Statistical significance was determined by a Student's *t*-test (****p*<0.001). (b, c, d) qPCR analysis showing induction of *MtPLATZ1* (b) and repression of *EMA1* (c) and *MtAAMT1* (d) in three independent *MtPLATZ1*^{OE} (OE) hairy root lines compared to three independent control (CTR) hairy root lines. Error bars indicate SEM (n = 3). Statistical significance was determined by a Student's *t*-test (***p*<0.01, ****p*<0.001). (e) Transient expression assay in tobacco protoplasts showing no relevant transcriptional repression of the 2000-bp *MtAAMT1* promoter (pAAMT1) driving *fLUC* expression by co-transfection of the protoplasts with an effector plasmid expressing *MtPLATZ1*. Values in the y-axis are normalized fold changes in log scale relative to protoplasts co-transfected with the reporter construct and a pCaMV35S:GUS (GUS) control plasmid. Error bars indicate SEM; n = 8 biological replicates. Statistical significance was determined by a Student's *t*-test (****p*<0.001). (f-h) qPCR analysis showing transcriptional response of *EMA1* (f), *MtAAMT1* (g), and *MtPLATZ1* (h) in *M. truncatula* seedlings treated for two or 24 hours with 100 μM of methyl anthranilate (MeAA). Error bars indicate SEM; n = 3 biological replicates. Statistical significance was determined by a Student's *t*-test (**p*<0.05, ***p*<0.01, ****p*<0.001).

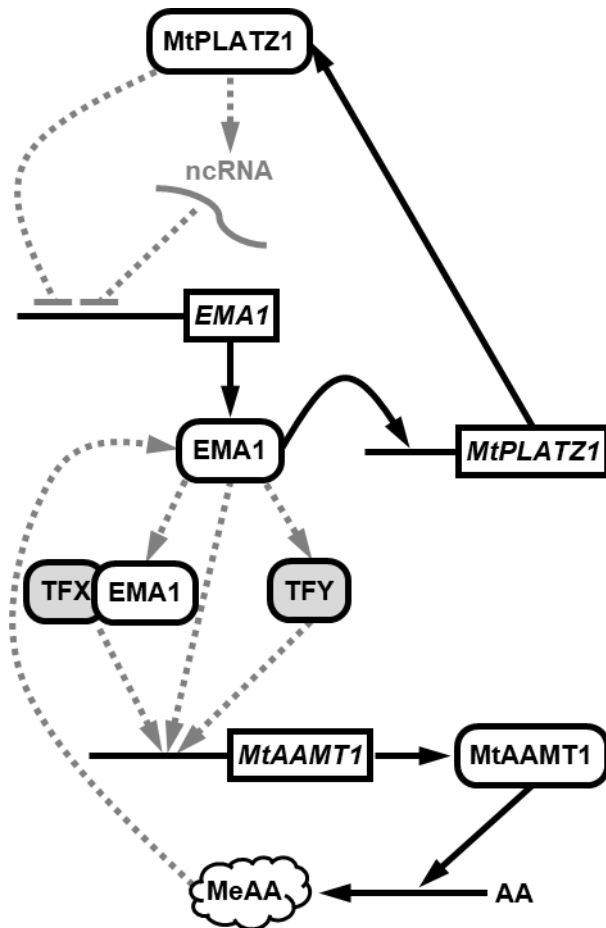


Figure 7. Tentative regulatory model for the role of EMA1 and MtPLATZ1 in the regulation of VOC emission from *M. truncatula* hairy roots. EMA1 might directly activate transcription of *MtAAMT1* through binding of *cis*-elements in gene sequences outside the 2000-bp promoter region currently assessed in the transactivation assays or through interaction with a yet unknown transcription factor (TFX), or modulate *MtAAMT1* expression indirectly by activating transcription of a yet unknown direct regulator of *MtAAMT1* that we could not readily identify from our transcriptome data set (TFY). EMA1 directly activates *MtPLATZ1* transcription, which might trigger a negative feedback loop repressing *EMA1* expression either by directly binding the *EMA1* promoter or through activating the expression of a yet elusive repressing ncRNA. The biosynthesis of methyl anthranilate (MeAA) from anthranilic acid (AA) by *MtAAMT1* might trigger an amplification loop that further boosts methyl anthranilate production. Full and dotted arrows indicate demonstrated and hypothetical molecular interactions, respectively.

SUPPORTING INFORMATION

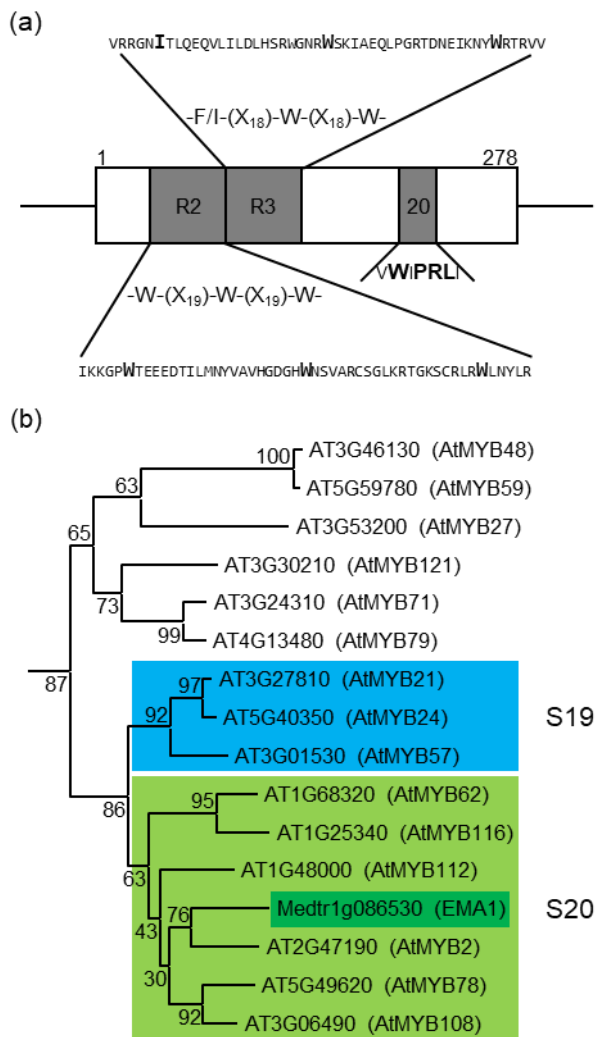


Figure S1. EMA1 belongs to the R2R3-MYB proteins subgroup 20. (a) Schematic representation of the EMA1 protein and its domain structures. (b) Fragment of the Neighbor Joining phylogenetic tree showing the relation of EMA1 with the *Arabidopsis* R2R3-MYB proteins. Subgroup 19 (S19) and 20 (S20) of the R2R3-MYB proteins are encased in blue and green boxes, respectively.

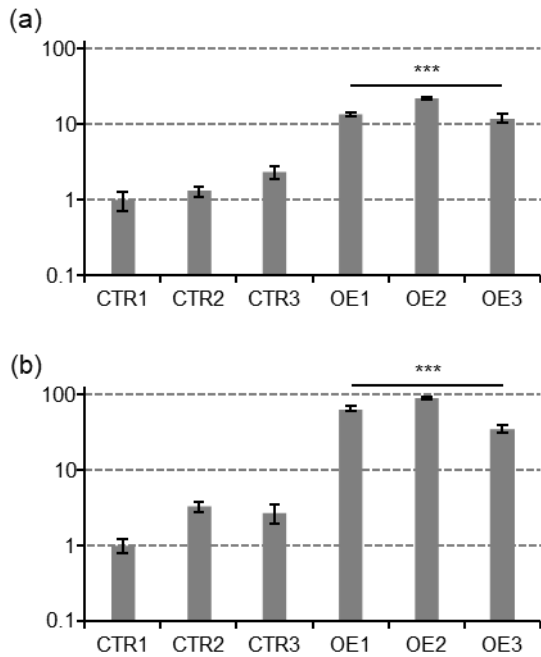


Figure S2. Accumulation of FGM and MGM in EMA1^{OE} lines. (a, b) Normalized ion current of FGM (a) and MGM (b) in three control (CTR) and three EMA1^{OE} (OE) lines. Error bars indicate SEM; n = 5 technical replicates. Statistical significance was determined by a Student's *t*-test with Welch correction (***)p<0.001).

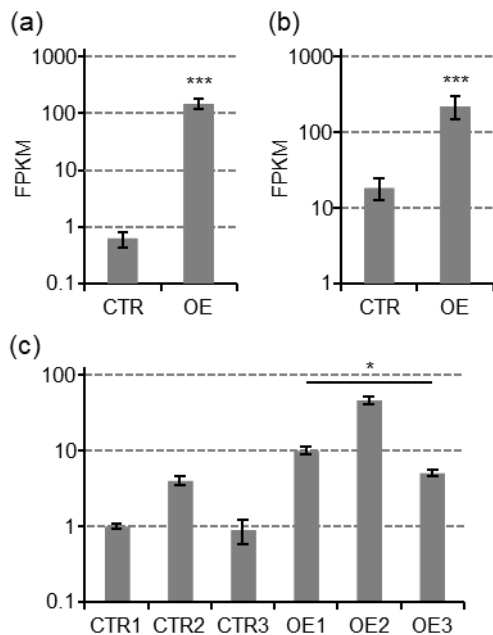


Figure S3. The expression of *Medtr4g018820* is increased in EMA1^{OE} lines. (a, b) RNA-Seq revealed an increased expression of *EMA1* (a) and *Medtr4g018820* (b) in EMA1^{OE} hairy root lines (OE) as compared to control (CTR) hairy root lines. The average FPKM values of three independent lines were plotted. Error bars indicate SEM; n = 3 technical replicates. Statistical significance was determined by the Cuffdiff program of the Cufflinks software package (***)p<0.001). (c) qPCR analysis showing increased levels of *Medtr4g018820* transcript levels in three independent EMA1^{OE} (OE) hairy root lines compared to three independent control (CTR) hairy root lines. Error bars indicate SEM; n = 3 technical replicates. Statistical significance was determined by a Student's *t*-test (*p<0.05).

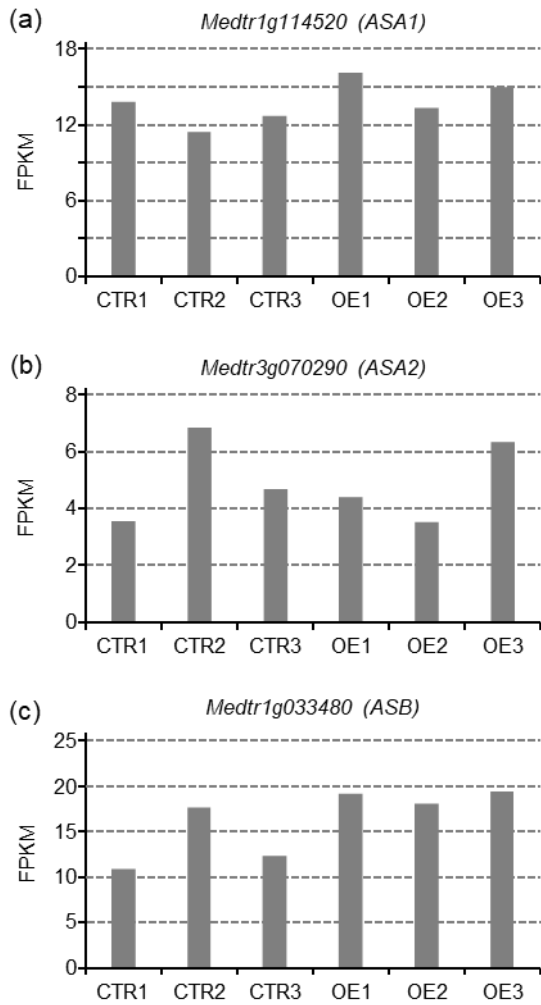


Figure S5. Expression of anthranilate synthase encoding genes in control and EMA1^{OE} lines. (a-c) RNA-Seq analysis of three independent control (CTR) and EMA1^{OE} (OE) hairy root lines indicated the expression of ASA1, ASA2 and ASB was not significantly increased in the EMA1^{OE} hairy root lines.

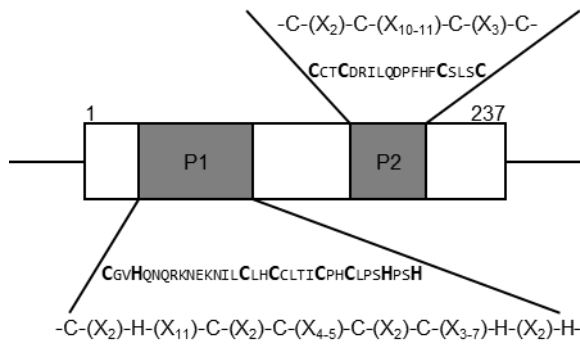


Figure S7. The PLATZ transcription factor family. Schematic representation of the MtPLATZ1 protein and its domain structures.

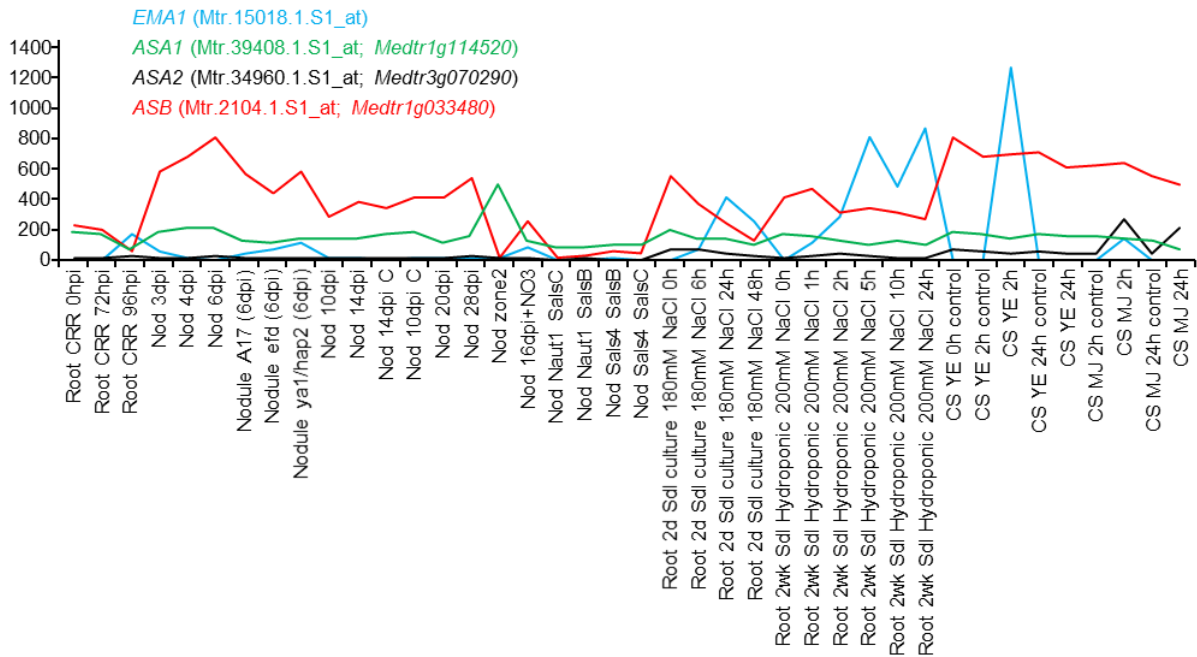


Figure S8. Expression of *EMA1*, *ASA1*, *ASA2*, and *ASB* in a selected set of conditions of the *M. truncatula* gene expression atlas. *EMA1* and the anthranilate synthase genes are not co-regulated. See <https://mtgea.noble.org/v3/> for more information on the samples and conditions.

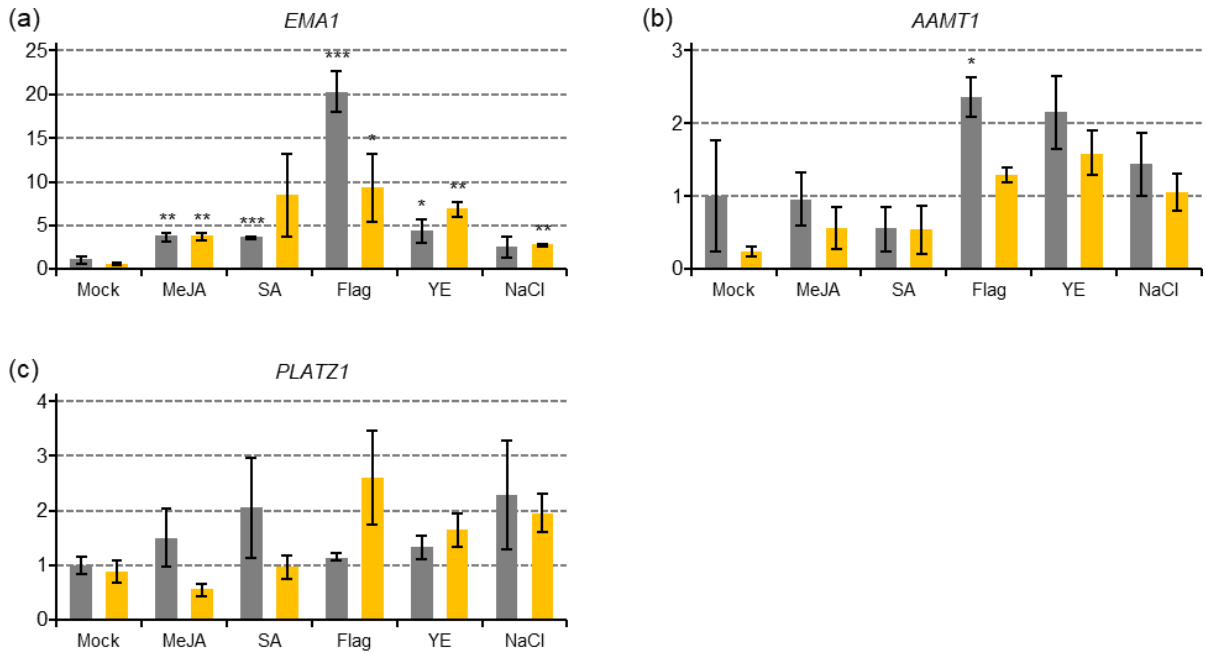


Figure S9. Expression of *EMA1* in *M. truncatula* seedlings treated with different elicitors. (a-c) qPCR analysis showing transcript levels of *EMA1* (a), *MtAAMT1* (b), and *MtPLATZ1* (c) in *M. truncatula* seedlings treated for two (grey bars) or 24 (orange bars) hours with methyl jasmonate (100 μ M; MeJA), salicylic acid (100 μ M; SA), Flag 22 (1 μ M; Flag), yeast elicitor (3% w/v; YE) or salt (200 μ M; NaCl). Error bars indicate SEM; n = 3 biological replicates. Statistical significance was determined by a Student's *t*-test (*p<0.05, **p<0.01, ***p<0.001).

Data S1. Identification of *M. truncatula* isoflavonoids.

Separate Word file.

Table S1. List with genes with significantly altered expression in the EMA1^{OE} lines compared to the CTR lines.

Separate Excel file.

Table S2. List with 68 genes with significantly altered expression in the EMA1^{OE} lines compared to additional control lines.

Separate Excel file.

Table S3. Expression of genes involved in *M. truncatula* (iso)flavonoid biosynthesis.

Separate Excel-file.

Table S4. List of 8-mer sequences with E-scores above 0.45 and the classification of the MBS motif.

8-mer	8-mer	E-score	Z-score	Motif
ACCTAACT	AGTTAGGT	0.49882	10.9113	MBSIIg
GTTAGGTA	TACCTAAC	0.49851	10.6629	MBSIIg
ACCTAACA	TGTTAGGT	0.49393	8.6580	MBSIIg
ACCTAACC	GGTTAGGT	0.49336	8.2307	MBSIIg
AGTTAGGC	GCCTAACT	0.49183	7.9543	MBSIIg
AACCTAAC	GTTAGGTT	0.49103	7.7969	MBSIIg
GACCTAAC	GTTAGGTC	0.49086	7.2176	MBSIIg
GTTAGGCA	TGCCTAAC	0.48787	6.9881	MBSIIg
AAGTTAGG	CCTAACTT	0.48721	5.4575	MBSIIg
AATTAGGT	ACCTAATT	0.48681	7.0184	MBSIIg
ATTAGGTA	TACCTAAT	0.48577	6.6886	MBSIIg
ATACCTAA	TTAGGTAT	0.48399	6.2948	MBSIIg
CACCTAAC	GTTAGGTG	0.48376	6.3430	MBSIIg
TTACCTAA	TTAGGTAA	0.48122	5.7115	MBSIIg
CCTAACTA	TAGTTAGG	0.48078	5.5763	MBSIIg
CTACCTAA	TTAGGTAG	0.47436	4.6670	MBSIIg
GGTAGGTA	TACCTACC	0.47293	5.9099	MBSIIg
ACCTAACG	CGTTAGGT	0.47191	5.5618	MBSIIg
ACCTAATC	GATTAGGT	0.47147	5.8980	MBSIIg
CCTAACTC	GAGTTAGG	0.46944	4.5599	MBSIIg
ACCAAAC	AGTTTGGT	0.46858	5.4531	MBSIIg
GTTTGGTA	TACCAAAC	0.46806	5.5074	MBSIIg
ATGTTAGG	CCTAACAT	0.46390	4.6760	MBSIIg
GTACCTAA	TTAGGTAC	0.46307	4.9679	MBSIIg
ACCTACCT	AGGTAGGT	0.46304	5.1054	MBSIIg
AGACCTAA	TTAGGTCT	0.45958	4.3635	MBSIIg
CGCCTAAC	GTTAGGCG	0.45814	4.7776	MBSIIg
GTTTCGGTA	TACCGAAC	0.45803	4.8150	MBSIIg
GCCTAACA	TGTTAGGC	0.45747	5.1042	MBSIIg
ATACCTAC	GTAGGTAT	0.45643	4.9044	MBSIIg
CAGTTAGG	CCTAACTG	0.45526	4.0778	MBSIIg
AAGTAGGT	ACCTACTT	0.45439	5.2036	MBSIIg
GCCTAACC	GGTTAGGC	0.45410	4.9853	MBSIIg
ATTAGGTC	GACCTAAT	0.45346	4.5130	MBSIIg
AATGTTGC	GCAACATT	0.45322	4.7658	MBSII
ACCGAACT	AGTTCGGT	0.45316	4.0088	MBSIIg

Table S5. Primers used in this study.

Nr	Description	Sequence
1142	Fw: qPCR control ELFa	ACTGTGCAGTAGTACTTGGTG
1143	Rv: qPCR control ELFa	AAGCTAGGAGGTATTGACAAG
1144	Fw: qPCR control 40S	GCCATTGTCTGAATTTGATGCTG
1145	Rv: qPCR control 40S	TTTTCTACCAACTTCAAAACACCG
1431	Fw: AttB1-EMA1	<u>GGGGACAAGTTTGTACAAAAAAGCAGGCT</u> CCATGGATACTAA TTACAAAACC
1432	Rv: AttB2-EMA1	<u>GGGGACCACTTTGTACAAGAAAGCTGGGT</u> CTCMTAAATCATC AGCCAATTGTTGC
1605	Fw: qPCR EMA1	GGACAGAAGAGGAGGATACTATTC
1606	Rv: qPCR EMA1	AGACTTGTCTTGGAGAGTGATG
2466	Fw: AttB1-P _{MtAAMT1} 1000 bp	<u>GGGGACAAGTTTGTACAAAAAAGCAGGCT</u> TAGCACCCACACA ATAACAATCGC
2467	Fw: AttB1-P _{MtAAMT1} 2000 bp	<u>GGGGACAAGTTTGTACAAAAAAGCAGGCT</u> TATAGCTGCCACC ATACTTCTTC
2468	Rv: AttB2-P _{MtAAMT1}	<u>GGGGACCACTTTGTACAAGAAAGCTGGGT</u> ATTTTGTTCCTTAT CTTTCTTTC
2471	Fw: AttB1-MtAAMT1	<u>GGGGACAAGTTTGTACAAAAAAGCAGGCT</u> TAATGGAAGTAG CTCAAGTACTACCC
2472	Rv: AttB2-MtAAMT1	<u>GGGGACCACTTTGTACAAGAAAGCTGGGT</u> ATCMTGCTTTTCT AGTCATCATTAGGG
2592	Fw: qPCR MtAAMT1	CTAACTATTATCCATCTCCAT
2593	Rv: qPCR MtAAMT1	CCACATTGTATCCATCAT
2594	Fw: qPCR MtPLATZ1	TCAGGCATATACGATTAACG
2595	Rv: qPCR MtPLATZ1	TTGGCAGCAGTAGTAGTA
2786	Fw: AttB1-MtPLATZ1	<u>GGGGACAAGTTTGTACAAAAAAGCAGGCT</u> TAATGAGAGGAA GTGGAAGTGACCC
2787	Rv: AttB2-MtPLATZ1	<u>GGGGACCACTTTGTACAAGAAAGCTGGGT</u> ACTAGATTAGAGG AGCTCTCTTAGG
2793	Fw: AttB1-P _{MtPLATZ1}	<u>GGGGACAAGTTTGTACAAAAAAGCAGGCT</u> TAATTTGGTTAGC TTCGGTTTGGAC
2795	Rv: AttB2-P _{MtPLATZ1}	<u>GGGGACCACTTTGTACAAGAAAGCTGGGT</u> AGTCTCACTCTAC AACACCACTTTG
2813	Fw: AttB1-P _{EMA1}	<u>GGGGACAAGTTTGTACAAAAAAGCAGGCT</u> TAATTAATGGAAG CATGTAATTAC
2815	Rv: AttB2-P _{EMA1}	<u>GGGGACCACTTTGTACAAGAAAGCTGGGT</u> AGTTTGTTACACT CACAGTTATAC
3080	Fw: AttB1-P _{MtPLATZ1} +MRE	<u>GGGGACAAGTTTGTACAAAAAAGCAGGCT</u> TAAGAAAAATGA AAAACAATCCTCC

Nr	Description	Sequence
3081	Fw: AttB1-P _{MiPLATZI} -MRE	<u>GGGGACAAGTTTGTACAAAAAAGCAGGCTTATTCAGTTGACA</u> TAAACAGAAAAC
3082	Fw: P _{MiPLATZI} MUT	CAATCCTCCTtctagagagctcgagtcCCAAACCATTTCAGTTGACATAA ACAG
3083	Rv: P _{MiPLATZI} MUT	GAATGGTTTGGgactcgagctctctagaAGGAGGATTGTTTTTCATTTTT CTTAC
3371	Fw: P _{MiPLATZI} Y1H	<u>GGGGACAAC TTTGTATAGAAAAGTTGCTAAGCTTAAAGTAAT</u> GATGAGTAAG
3372	Rv: P _{MiPLATZI} Y1H	<u>GGGGACTGCTTTTTTTGTACAAACTTGCAAGCTTTGAACTAAAG</u> TTTTCTG
3373	P1 3x MRE-box	GAAAAGTTGCTAAGCTTCTAACCTAACCTAACCTAACCTCGA GGAGAATCCTGGCCCA
3374	P2 3x MRE-box	GGTTAGGTTAGGTTAGGTTAGTGGGCCAGGATTCTCCTCGA
3375	P3 3x MRE-box	CTAACCTAACCTAACCTAACCTGCTAACATGCGGTGACGT
3376	P4 3x MRE-box	CAAAC T TGCCAGCTGGGTTAGGTTAGGTTAGGTTAGACGTCA CCGCATGTTAGCAG
3377	P5 3x MRE-box	GGGGACAAC T TTGTATAGAAAAGTTGCTAAGCTT
3378	P6 3x MRE-box	GGGGACTGCTTTTTTTGTACAAACTTGCCAGCTG

The underlined sequences correspond to the Gateway sequences; the sequences in lowercase represent mutated sequences.